Modeling Earth Systems and Environment
https://doi.org/10.1007/s40808-024-02128-7

ORIGINAL ARTICLE

Optimal control and cost-effectiveness analysis for a tuberculosis vaccination model with two latent classes

Raymond Fosu Appiah[1] · Zhen Jin[1] · Junyuan Yang[1] · Joshua Kiddy K. Asamoah[2,3]

Received: 16 March 2024 / Accepted: 4 August 2024

Abstract

Tuberculosis (TB) persists as a significant public health challenge in many regions, including Ghana. Effective treatment strategies are crucial in controlling the spread of TB, particularly in populations with diverse characteristics. This study delves into designing an optimal treatment strategy for the TB vaccination model, considering two latent classes based on Ghanaian data. We estimate and analyze the parameters to study TB dynamics based on the reproduction numbers of the two latent classes. We look into how sensitive the parameters are to see the transmission dynamics of the slow latent class of TB infectious with drug-sensitive strains and the rapid latent class of TB infectious with drug-resistant strains. Using optimal control theory techniques, we devise an optimal control strategy with a cost–benefit analysis to minimize TB incidence and maximize vaccination coverage within budget constraints. This strategy aims to guide policymakers in allocating resources efficiently to control the spread of TB. The results of this work give in-depth knowledge about the dominance of the two strains of TB transmission and provide insights into the design of effective vaccination and treatment programs. By tailoring interventions to the population's specific needs, we can work towards reducing the burden of TB worldwide.

Keywords Tuberculosis · Slow latent class · Fast latent class · Optimal control analysis · Cost-effectiveness

Introduction

Over the years, the prevalence of tuberculosis (TB), particularly in developing nations, presents a significant public health concern due to its spread. This is attributed to the endemic nature of the causative agents, poverty, drug-resistant tuberculosis and ineffective diagnostic techniques. Some of these factors contribute to the difficulty in controlling tuberculosis in Africa (Adebisi et al. 2019). Tuberculosis (TB) is one of the top ten leading causes of death worldwide, which affects about one-third of the world's population each year, as recorded by the World Health Organization (WHO) health statistics (WHO 2015). Tuberculosis (TB) induced death in 2015 was about 1.4 million out of 10.4 million reported worldwide (WHO 2016). Africa is one of the continents with a comparatively higher disease prevalence than other continents (Snider et al. 1994; WHO 2013). Ghana reported 148 cases of tuberculosis per 100,000 people, with a 36% death rate associated with the disease (WHO 2018).

Chemotherapy has been the mainstay of apparent control programs for TB due to vaccine inefficacy (WHO 2016). Compared to infectious sensitive TB patients who have not yet acquired the disease, the antibiotic treatment for an active TB patient (with drug-sensitive strain) takes a lot longer and costs more (Reichman and Hershfield 2000). One of the most dangerous public health issues currently plaguing society is antibiotic-resistant tuberculosis (TB), which can develop from noncompliance with medication treatments in addition to increasing the risk of relapse (WHO 2018). According to a World Health Organization report (WHO 2018), if nations do not move swiftly to tighten their control over tuberculosis, the multidrug-resistant strains that have cost Russia and New York City more than $1 billion and hundreds of lives each will continue to surface in other countries (WHO 2018; Chaulet 1983).

✉ Zhen Jin
jinzhn@263.net

✉ Junyuan Yang
yjyang66@sxu.edu.cn

[1] Complex Systems Research Center, Shanxi University, Taiyuan 030006, China

[2] Department of Mathematics, Saveetha School of Engineering SIMATS, Chennai, India

[3] Department of Mathematics, Kwame Nkrumah University of Science and Technology, Kumasi, Ghana

Published online: 11 September 2024

Over the years, there has been an increased interest in using mathematical models to study the patterns of infectious diseases. This is because these models help better understand how diseases spread and conveniently summarise epidemiological data (Blower et al. 1996). As a result, the infection spreads and is increasingly anticipated as future outbreaks occur, and robust decisions regarding managing the underlying illness are made (Castillo-Chavez and Feng 1997). Models used to investigate the spread of infectious diseases are known as dynamic epidemiological models. Since there may be some variations in infection rates among populations. Disease modellers attempt to account for these variations when creating mathematical models for epidemics. This approach produces a class of models known as compartmental models.

Wireko et al. (2024) conducted a study on the analysis of measles using accurate data, focusing on non-optimal and optimal fractional control methods. By employing numerical simulations and sensitivity analysis, they determined the most effective control mechanisms that balance the effectiveness of interventions, allocation of resources, and societal costs. Appiah et al. (2024a; b) introduced a mathematical model that examines the interaction between two tuberculosis strains and COVID-19 immunisation. The study also includes a cost-effectiveness analysis. Appiah et al. (2024a; b) surveyed the cost–benefit analysis of the COVID-19 vaccination model. They incorporated various levels of infectivity reduction and used data from Ghana. Addai et al. (2023) examined a deterministic model exploring Marburg virus transmission dynamics. The model considers the influence of public health education and is now being developed and analysed. Using a fractional-based approach, the Caputo fractional-order derivative expands upon the conventional integer model. The model's positive nature and limited scope are also acquired.

To study the co-dynamics of tuberculosis (TB) and SARS-CoV-2, Rwezaura et al. (2022) created a mathematical model that incorporates epidemiological aspects. The sub-models exhibit local asymptotic stability when the reproduction numbers for the disease-free and endemic equilibria are less than one. After doing a bifurcation analysis on the TB-only sub-model, it was demonstrated that the sub-model passes through forward bifurcation. From February 11, 2021, through August 26, 2021, the model is fitted to Indonesia's total confirmed daily SARS-CoV-2 cases. Considering environmental pollution and safe burier, Adu et al. (2024) analyse a non-linear mathematical model of Ebola. The suggested model is proven to be well-posed, bounded, and non-negative. We find the Ebola reproduction number, the Ebola-free equilibrium, and the Ebola-present equilibrium. The Ebola reproduction number is subjected to a sensitivity study to determine which factors impact its output. Addai et al. (2024) developed and evaluated a mathematical model for transmitting food-borne diseases using a population of flies and humans as a model. Using the Caputo operator, we investigate how internet meal delivery services and government regulations affect the spread of food-borne illnesses. Key features examined by the suggested model include sensitivity analysis, fundamental reproduction number, positivity, boundedness, disease-free equilibrium, and basic parameters. An Ebola epidemic model was developed by Wang et al. (2023). This model considers several factors, including the scarcity of medical resources, the decline in immunity, and the possibility of quarantining and tracking vulnerable persons. At the same time, it has been demonstrated that the disease-free equilibrium is stable. Bifurcation and the presence of several endemic equilibria are also inferred. The PRCC analysis then reveals that the parameter (the rate of incineration or burial of corpses) is most strongly connected to the control reproduction number. An EVD model for the incubation period was developed by Ren and Xu (2024) and includes four gearbox modes and a time delay. By utilising dynamical analysis, they confirm that eradicating sick animals from their environments is crucial. Without considering the source of infection, we obtain the fundamental reproduction number. When the basic reproduction number is less than one, the model achieves an attractive disease-free equilibrium on a global scale. However, the disease becomes endemic when the basic reproduction number increases beyond one. Asamoah et al. (2023) examined the dynamics of Gonorrhoea, explicitly focusing on the positively invariant and limited portions of the model. The computation of the expression for the secondary infection of Gonorrhoea in a structured population is performed. The Pontryagin's maximum principle is employed to derive the optimal system for the given mathematical model.

Seidu et al. (2023) developed a non-linear deterministic model to analyse cholera dynamics while considering two distinct groups of persons categorised by their hygiene levels. These individuals are classified into low-risk and high-risk categories based on their level of personal hygiene, with low-risk referring to those with good personal hygiene and high-risk referring to those with very low personal hygiene. The model exhibits two distinct fixed points that are mutually exclusive: the cholera-free equilibrium and the cholera-persistent equilibrium. This suggests the occurrence of forward bifurcation. He et al. (2023) studied a hierarchical intervention scheme based on epidemic severity in a community network. The paper by Abidemi et al. (2022) explores creating and examining a non-linear mathematical model that describes the spread and management of dengue disease in both human and mosquito populations. A twelve-dimensional set of ordinary differential equations controls the model. It represents the group of symptomatic infected humans with severe dengue symptoms and the population of mosquitoes infected with Wolbachia. Moore et al.

(2022) examined how the timing of diagnosis, whether done promptly or with a delay, influenced the transmission of COVID-19 in Ghana during the early stage of the outbreak. They analysed data reported between March 12 and June 19, 2020. The projected value of the basic reproduction number, R0, for the suggested model, is 1.04. They proposed that decreasing the influx of new individuals into the country or reducing the inflow of individuals between communities will lower the basic reproduction number and hence decrease the number of secondary infections (resulting in several peaks of the infection).

Some previous TB models have included drug treatment and vaccination and have examined the prevalence of the disease. These models were predictive and attempted to calculate the basic reproduction number. Since their discussions are predicated on the prevalence of the disease at equilibria, these models did not consider time-dependent control strategies. For HIV models, time-dependent control strategies have been researched (Fister et al. 1998; Kirschner et al. 1997). Both methods of examining control strategies yield insightful theoretical findings that can be applied to the recommendation or creation of programs to control epidemics. Different objective criteria may be adopted depending on the selected goals.

A deterministic model splits a heterogeneous population into a finite number of homogeneous subpopulations. Next, ordinary differential equations (ODE) are used to model the epidemic dynamics deterministically with movement within and between subpopulations. There is a long history of using the deterministic approach to model infectious diseases. Numerous infectious diseases, including flu, chickenpox, measles, etc., have been extensively studied using these models in various settings (Zhilan et al. 2000). Theoretical outcomes from deterministic models include thresholds, replacement numbers, contact numbers and the basic reproduction number. These models aid nations, areas, and societies in developing appropriate countermeasures to lower the likelihood of infection by pathogens (Hethcote 2000).

Several classes of compartmental models have been used in studies to investigate TB infection from a modelling perspective (Castillo-Chavez and Feng 1998; Rieder et al. 1989; Blower et al. 1998; Blower and Gerberding 1998). However, modelling the effect of the overall TB infection dynamics on the exposed individuals differs from that of the susceptible-infected-recovered (SIR) models, which are frequently adopted when the latent stage of the infection is ignored. Most TB studies that used the SEIR model investigated global stability at the incubation, infectious and recovered stages using either non-sequential occurrence rate or infectious drive (Castillo-Chavez and Song 2004; Li and Jin 2005; Li et al. 1995). However, compared to the SIR model, only a few works have been conducted in Ghana utilising basic models in the context of tuberculosis infection because there is little knowledge about the possible carriers in society at any given time (Dontwi et al. 2014).

Based on the two-strain model created by Castillo-Chavez and Feng (1997), we examine optimal strategies related to case holding and case finding, public education and vaccination, and the cost associated with them in this work. This model assumes that people who have latent TB become active at a specific rate. Additionally, it assumes that some treated patients with active tuberculosis will not complete their course of treatment while some of them develop drug-resistant tuberculosis. Four control mechanisms for public education, vaccination, case finding and case-holding efforts are incorporated into this model.

The subsequent sections of this work are presented as follows; "Method" presents the detailed framework of the epidemiological model and the definition of the parameters and variables. The method also contains the analysis of the model's positivity of solutions, computation of the effective reproduction number and stability of the model. "Numerical method" presents the model parameters estimation and sensitivity analysis of the parameters. "Results" presents the optimal control analysis using the numerical method. "Discussion" presents the cost–benefit analysis of the control interventions. Lastly, the "Conclusion" section summarises the findings and provides suggestions for further research.

Methods

Framework of the tuberculosis (TB) vaccination model

The TB vaccination model is designed by considering two strains: the slow latent class with a drug-sensitive (DS) strain of TB and the fast latent class with a drug-resistant (DR) strain of TB. The proposed epidemiological model is designed by dividing the compartments into seven distinct classes, thus $S(t)$: Susceptible class, $V(t)$: Vaccinated class, $E_s(t)$: Slow latent class exposed to drug-sensitive (DS) strain TB but not infectious, $I_s(t)$: Slow infectious class with drug-sensitive (DS) TB, $E_f(t)$: Fast latent class infected exposed to drug-resistant (DR) strain of TB but not infectious, $I_f(t)$: Fast infectious class with drug-resistant (DR) strain TB and $T(t)$: Treated class. The model is illustrated based on the following; $S(t)$ and $V(t)$ compartments recruit individuals by $(1-b)\Lambda$ and $b\Lambda$ respectively where b belonging to $[0, 1]$ represents the proportion of newborns vaccinated and $1-b$ represents newborns not vaccinated. The individuals in $S(t)$ and $V(t)$ are infected by the two strains at the rate of $\beta_s SI_s, \beta_f SI_f$ and $\vartheta\beta_s VI_s, \vartheta\beta_f VI_f$ respectively where ϑ belonging to $[0, 1]$ denotes the vaccine protection rate. If $\vartheta = 0$ then the vaccination protection is 100% efficient, $\vartheta = 1$ denotes vaccine efficiency is 0 and the immunity

waning rate coefficient in the vaccinated host is φ which is given as $\varphi \geq 1$. We consider that a proportion of a and $1-a$ of the individuals in $S(t)$ enter the slow latent classes $I_s(t)$ and $E_s(t)$ respectively and a proportion of a and $1-a$ of the individuals in $V(t)$ enter $I_s(t)$ and $E_s(t)$ respectively likewise the fast latent classes $I_f(t)$ and $E_f(t)$. The respective rate of death due to TB disease is given as d_i where $i = 1,2,3,4$ for $E_s(t), I_s(t), E_f(t)$ and $I_f(t)$ individuals. The individuals in $E_s(t)$ and $E_f(t)$ leave these compartments and become infectious with $I_s(t)$ and $I_f(t)$ at the rate of δ_s and δ_f respectively. The individuals in $I_s(t)$ compartment progress to different compartments in the following ways; individuals identified to be infected are moved to $T(t)$ at the rate of α_t for prophylaxis, a proportion of g moves to $E_s(t)$ at the rate of $g\alpha_s$ due to self-cure, proportion of k moves to $E_f(t)$ at the rate of $k\alpha_s$ due to self cure, proportion of n moves to $I_f(t)$ at the rate of $n\alpha_s$ due to unsuccessful prophylaxis and proportion of $1-(g+k+n)$ progresses to $T(t)$ at $(1-(g+k+n))\alpha_s$ rate to undergo prophylaxis where g, k, n all belong to [0,1) and $g+k+n \leq 1$ represents the fraction of individuals who did not complete their prophylaxis when infected with drug-sensitive (DS) strain TB. Also, a proportion of h moves to $E_f(t)$ at the rate of $h\alpha_f$ due to self cure and proportion of $1-h$ progresses to $T(t)$ at the rate of $(1-\mathrm{h})\alpha_f$ to undergo prophylaxis where h all belongs to [0,1]. The individuals in $T(t)$ compartment progress to different compartments in the following ways; a proportion of m moves to $E_s(t)$ and $E_f(t)$ at the rate of $\frac{m\varepsilon\beta_s TI_s}{N}$ and $\frac{m\varepsilon\beta_f TI_f}{N}$ respectively upon successful prophylaxis, where as $1-m$ moves to $I_s(t)$ and $I_f(t)$ at the rate of $\frac{(1-m)\varepsilon\beta_s TI_s}{N}$ and $\frac{(1-m)\varepsilon\beta_f TI_f}{N}$ respectively due to failure of prophylaxis where $1-m$ accounts for the proportion of individuals who develop the drug-resistant (DR) strain TB. The meanings of the rest of the parameters associated with the model are given in the table below. Optimal control efforts $U_p(t), U_v(t), U_s(t)$ and $U_f(t)$ would be applied and explained in detail in the subsequent sections.

The total population $N(t)$ is defined based on the flowchart diagram Fig. 1 as;

$$N(t) = S(t) + V(t) + E_s(t) + I_s(t) + E_f(t) + I_f(t) + T(t). \quad (1)$$

We formulate the following set of nonlinear ordinary differential equations that describe the nature of the model.

$$\begin{cases} \frac{dS}{dt} = (1-b)\Lambda + \varphi V - \lambda S - \mu S, \\ \frac{dV}{dt} = b\Lambda - \lambda\vartheta V - z_1 V, \\ \frac{dE_s}{dt} = \frac{[(1-a)(S+\vartheta V)+m\varepsilon T]\beta_s I_s}{N} + g\alpha_s I_s - z_2 E_s, \\ \frac{dI_s}{dt} = \frac{[a(S+\vartheta V)+(1-m)\varepsilon T]\beta_s I_s}{N} + \delta_s E_s - z_3 I_s, \\ \frac{dE_f}{dt} = \frac{[(1-a)(S+\vartheta V)+m\varepsilon T]\beta_f I_f}{N} + k\alpha_s I_s + h\alpha_f I_f - z_4 E_f, \\ \frac{dI_f}{dt} = \frac{[a(S+\vartheta V)+(1-m)\varepsilon T]\beta_f I_f}{N} + n\alpha_s I_s + \delta_f E_f - z_5 I_f, \\ \frac{dT}{dt} = \alpha_e E_s + (1-(g+k+n))\alpha_s I_s + (1-h)\alpha_f I_f - (\mu+\varepsilon\lambda)T, \end{cases} \quad (2)$$

where $\lambda = \frac{(1-a)(\beta_s I_s + \beta_f I_f)}{N}$, $z_1 = \mu + \varphi$, $z_2 = \mu + d_1 + \delta_s + \alpha_e$, $z_3 = \mu + d_2 + \alpha_s$, $z_4 = \mu + d_3 + \delta_f$, $z_5 = \mu + d_4 + \alpha_f$. With initial conditions $S(0) \geq 0, V(0) \geq 0, E_s(0) \geq 0, I_s(0) \geq 0, E_f(0) \geq 0, I_f(0) \geq 0, T(0) \geq 0$. All the parameters of system (2) are nonnegative.

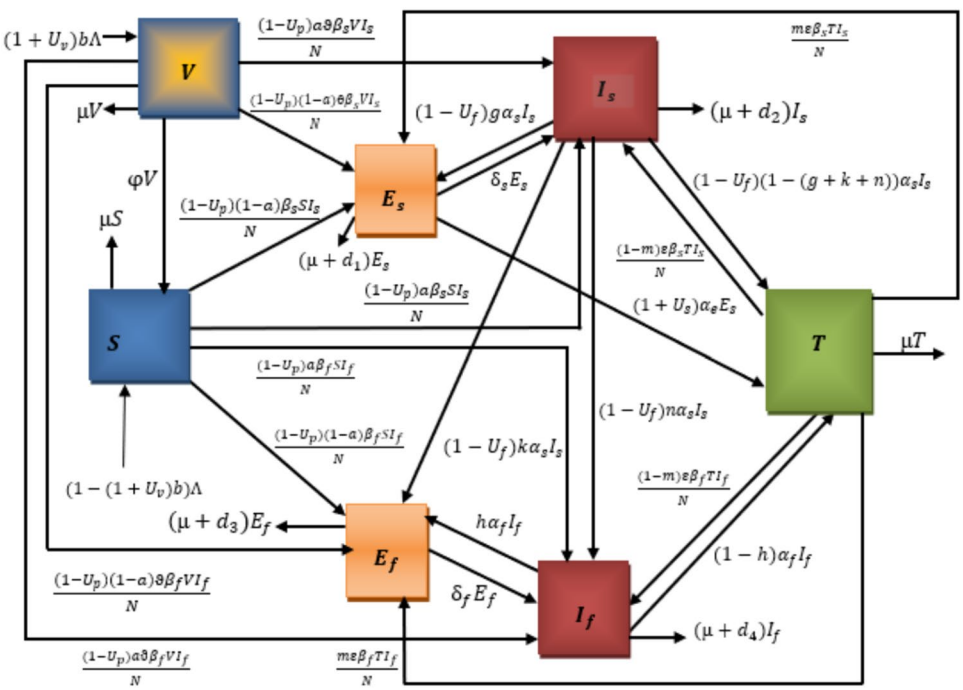

Fig. 1 Flowchart of the tuberculosis vaccination model

Positivity of solutions for the tuberculosis (TB) vaccination model

The model (2) variables and parameters are nonnegative since it is designed based on population with TB and it follows.

Theorem 1 *The model (2) and its solutions and initial values are nonnegative such that* $\{S(t)>0, V(t)>0, E_s(t)>0, I_s(t)>0, E_f(t)>0, I_f(t)>0, T(t)>0\}$, *for* $t \geq 0$, *and bounded in the region* R_+^7.

Proof Let's consider the following instance that there exists an initial time t_i, such that

$\min\{Y(t_i)\} > 0$ and $\min\{Y(t)\} > 0$ for all $t \in [0, t_i)$.

Here,

$$Y(t) = S(t), V(t), E_s(t), I_s(t), E_f(t), I_f(t), T(t). \tag{3}$$

Then, from the above assumption, our initial value is given as, $\min\{Y(t_i)\} = S(t_i)$.

Therefore, $S(t_i) = 0$ and $S(t) > 0$ for all $t \in [0, t_i)$. However,

$$\frac{dS(t_i)}{dt} = (1-b)\Lambda + \varphi V - (\lambda+\mu)S(t_i) \geq (\lambda+\mu)S(t_i). \tag{4}$$

Then,

$$\int_0^{t_i} (\lambda+\mu)du > 0, S(t_i) \geq S(0). \tag{5}$$

This disputes the assumption $S(t_i) = 0$. Therefore, $S(t) > 0$ for all $t \geq 0$. This shows that all the solutions are positive for $t \geq 0$ in all other situations.

Theorem 2 *Let's consider* $(S(t)>0, V(t)>0, E_s(t)>0, I_s(t)>0, E_f(t)>0, I_f(t)>0, T(t)>0)$ *with initial state* $S(0), V(0), E_s(0), I_s(0), E_f(0), I_f(0), T(0)$ *for all the solutions remain bounded in* R_+^7 *in the region* $W = \{(S, V, E_s, I_s, E_f, I_f, T) \in R_+^7 : U \leq N(t)\}$.

Proof Let's consider the function below:

$$U = S(t) + V(t) + E_s(t) + I_s(t) + E_f(t) + I_f(t) + T(t). \tag{6}$$

Taking the derivative of U with respect to time is given as follows results.

$$U'(t) = S'(t) + V'(t) + E_s'(t) + I_s' + E_f' + I_f' + T'(t), \tag{7}$$

$$U'(t) = \Lambda - \mu U(t) - \left(d_1E_s + d_2I_s + d_3E_f + d_4I_f\right) \leq \Lambda - \mu U(t), \tag{8}$$

$$N'(t) = \Lambda - \mu N(t) - (d_1E_s + d_2I_s + d_3E_f + d_4I_f) \leq \Lambda - \mu N(t). \tag{9}$$

Then, integing of Eq. (9), the solution for $N(t)$ is derived as follows; $N(t) \leq \frac{\Lambda}{\mu}(1-e^{-\mu t}) + N(0)e^{-\mu t}$ for all t. Thus, $S(t) + V(t) + E_s(t) + I_s(t) + E_f(t) + I_f(t) + T(t)$ are bounded in $\left[0, \frac{\Lambda}{\mu}\right]$, for all t. Since $U(t) \leq 0$, then W is a set of positive invariant. Conversely, the system (2) is obtained in $0 \leq L(t) \leq N(t) + N(0)e^{-\mu t}$ and $W(0)$ is the initial state variable condition of $U(t)$. Therefore, if $t \to \infty, 0 \leq U(t) \leq N(t)$ shows that $U(t)$ is a set of positive invariant in the region R_+^7. Therefore, the proof is complete.

Disease-free equilibrium D_0 and effective reproduction number

The disease-equilibrium point, D_0 of the model is achieved by equating the system (2) to zero. At Disease-free equilibrium, we set $E_s = I_s = E_f = I_f = T = 0$ and the following results are obtained;

$$S_0 = \frac{\Lambda[(1-b)+\varphi/\mu]}{z_1}, V_0 = \frac{b\Lambda}{z_1}. \tag{10}$$

At disease-free equilibrium (DFE)

$$D_0 = \left(\frac{\Lambda[(1-b)+\varphi/\mu]}{z_1}, \frac{b\Lambda}{z_1}, 0,0,0,0,0\right). \tag{11}$$

The corresponding Jacobian matrix of system (2) evaluated at disease-free equilibrium $D_0 = (S_0, V_0, 0,0,0,0,0)$ to obtain the disease-free equilibrium Jacobian matrix J_{D_0} is given as;

$$J_{D_0} = \begin{pmatrix} -\mu & \varphi & 0 & -\frac{(1-a)\beta_s S_0}{N_0} & 0 & -\frac{(1-a)\beta_f S_0}{N_0} & 0 \\ 0 & -z_1 & 0 & -\frac{(1-a)\beta_s \vartheta V_0}{N_0} & 0 & -\frac{(1-a)\beta_f \vartheta V_0}{N_0} & 0 \\ 0 & 0 & -z_2 & \frac{(1-a)\beta_s[S_0+\vartheta V]}{N_0} + g\alpha_s & 0 & 0 & 0 \\ 0 & 0 & \delta_s & \frac{a\beta_s[S_0+\vartheta V_0]}{N_0} - z_3 & 0 & 0 & 0 \\ 0 & 0 & 0 & k\alpha_s & -z_4 & \frac{(1-a)\beta_f[S_0+\vartheta V_0]}{N_0} + h\alpha_f & 0 \\ 0 & 0 & 0 & n\alpha_s & \delta_f & \frac{a\beta_f[S_0+\vartheta V_0]}{N_0} - z_5 & 0 \\ 0 & 0 & \alpha_e & (1-(g+k+n))\alpha_s & 0 & (1-h)\alpha_f & -\mu \end{pmatrix}. \tag{12}$$

where $N_0 = S_0 + V_0$ using the Jacobian at the disease-free equilibrium D_0.

According to the explanation in (Shuai and van den Driessche 2013), the basic reproduction number is the spectral radius of the next generation operator $G = FV^{-1}$. For (2), we have the square matrix which has matrix F as

the new infections and matrix V as the transition elements of the infected classes.

$$F=\begin{pmatrix} 0 & \frac{(1-a)\beta_s[S_0+\vartheta V_0]}{N_0} & 0 & 0 \\ 0 & \frac{a\beta_s[S_0+\vartheta V_0]}{N_0} & 0 & 0 \\ 0 & 0 & 0 & \frac{(1-a)\beta_f[S_0+\vartheta V_0]}{N_0} \\ 0 & 0 & 0 & \frac{a\beta_f[S_0+\vartheta V_0]}{N_0} \end{pmatrix}, \tag{13}$$

$$V=\begin{pmatrix} z_2 & -g\alpha_s & 0 & 0 \\ -\delta_s & z_3 & 0 & 0 \\ 0 & -k\alpha_s & z_4 & -h\alpha_f \\ 0 & -n\alpha_s & -\delta_f & z_5 \end{pmatrix}, G=\begin{pmatrix} g_{11} & g_{12} & 0 & 0 \\ g_{21} & g_{22} & 0 & 0 \\ g_{31} & g_{32} & g_{33} & g_{34} \\ g_{41} & g_{42} & g_{43} & g_{44} \end{pmatrix}, \tag{14}$$

where

$$\begin{aligned} g_{11} &= \frac{(1-a)\beta_s\delta_s[S_0+\vartheta V_0]}{N_0(z_2z_3-g\alpha_s\delta_s)}, \\ g_{12} &= \frac{(1-a)\beta_s z_4[S_0+\vartheta V_0]}{N_0(z_2z_3-g\alpha_s\delta_s)}, \\ g_{21} &= \frac{a\beta_s\delta_s[S_0+\vartheta V_0]}{N_0(z_2z_3-g\alpha_s\delta_s)}, \\ g_{22} &= \frac{a\beta_s z_2[S_0+\vartheta V_0]}{N_0(z_2z_3-g\alpha_s\delta_s)}, \\ g_{31} &= \frac{(1-a)\beta_f\delta_s[S_0+\vartheta V_0](k\alpha_s\delta_f+n\alpha_s z_4)}{N_0(z_2z_3z_4z_5-g\alpha_s z_4z_5)}, \\ g_{32} &= \frac{(1-a)\beta_f[S_0+\vartheta V_0](k\alpha_s\delta_f z_2+n\alpha_s z_2z_4)}{N_0(z_2z_3z_4z_5-g\alpha_s z_4z_5)}, \\ g_{33} &= \frac{(1-a)\beta_f\delta_f[S_0+\vartheta V_0]}{N_0(z_4z_5-h\alpha_f\delta_f)}, \\ g_{34} &= \frac{(1-a)\beta_f z_4[S_0+\vartheta V_0]}{N_0(z_4z_5-h\alpha_f\delta_f)}, \\ g_{41} &= \frac{a\beta_f\delta_s[S_0+\vartheta V_0](k\alpha_s\delta_f+n\alpha_s z_4)}{N_0(z_2z_3z_4z_5-g\alpha_s z_4z_5)}, \\ g_{42} &= \frac{a\beta_f[S_0+\vartheta V_0](k\alpha_s\delta_f z_2+n\alpha_s z_2z_4)}{N_0(z_2z_3z_4z_5-g\alpha_s z_4z_5)}, \\ g_{43} &= \frac{a\beta_f\delta_f[S_0+\vartheta V_0]}{N_0(z_4z_5-h\alpha_f\delta_f)}, \\ g_{44} &= \frac{a\beta_f\delta_f z_4[S_0+\vartheta V_0]}{N_0(z_4z_5-h\alpha_f\delta_f)}. \end{aligned} \tag{15}$$

It is observed that, there is a positive matrix F and V has W-matrix with K-pattern. Then the effective reproduction number

$$R_e=\mathcal{P}\left(FV^{-1}\right)=\max\left\{R_s,R_f\right\}, \tag{16}$$

where

$$R_s=\frac{(1-a)\beta_s\delta_s[S_0+\vartheta V_0]}{N_0(z_2z_3-g\alpha_s\delta_s)}, R_f=\frac{(1-a)\beta_f\delta_f[S_0+\vartheta V_0]}{N_0(z_4z_5-h\alpha_f\delta_f)}. \tag{17}$$

Substituting N_0, S_0 and V_0 give the following results.

$$\begin{aligned} R_s &= \frac{(1-a)\beta_s\delta_s\left((1-b)+\frac{\vartheta\varphi}{\mu}\right)}{\left(z_2z_3-g\alpha_s\delta_s\right)\left((1-b)+\frac{\varphi}{\mu}\right)}, \\ R_f &= \frac{(1-a)\beta_f\delta_f\left((1-b)+\frac{\vartheta\varphi}{\mu}\right)}{\left(z_4z_5-h\alpha_f\delta_f\right)\left((1-b)+\frac{\varphi}{\mu}\right)}. \end{aligned} \tag{18}$$

where R_s is the reproduction number of the slow latent class infectious with drug-sensitivity (DS) strain of TB and R_f is the reproduction number of the fast latent class infectious with drug-resistant (DR) strain of TB.

Stability and existence of endemic equilibria

We focus on the existence and uniqueness of the endemic equilibrium points of model (2) as $D^*=\left(S^*,V^*,E_s^*,I_s^*,E_f^*,I_f^*,T^*\right)$. If $\varepsilon=0, R_s>R_f$ then, model (2) has $D^*=\left(S^*,V^*,E_s^*,I_s^*,E_f^*,I_f^*,T^*\right)$ as the unique endemic equilibrium. Setting system (2) to zero, we have the following results.

$$\begin{cases} (1-b)\Lambda+\varphi V^*-\lambda_1^{**}S^*-\mu S_s^*=0, \\ \Lambda b-\lambda_1^{**}\vartheta V^*-z_1V^*=0, \\ \frac{(1-a)\beta_sI_s^*[S^*+\vartheta V^*]+m\varepsilon\beta_iT^*I_s^*}{N^*}+g\alpha_sI_s^*-z_2E_s^*=0, \\ \frac{a\beta_sI_s^*[S^*+\vartheta V^*]+(1-m)\varepsilon\beta_iT^*I_s^*}{N^*}+\delta_sE_s^*-z_3I_s^*=0, \\ \frac{(1-a)\beta_fI_f^*[S^*+\vartheta V^*]+m\varepsilon\beta_iT^*I_f^*}{N^*}+k\alpha_sI_s^*+h\alpha_fI_f^*-z_4E_f^*=0, \\ \frac{a\beta_fI_f^*[S^*+\vartheta V^*]+(1-m)\varepsilon\beta_iT^*I_f^*}{N^*}+n\alpha_sI_s^*+\delta_fE_f^*-z_5I_f^*=0, \\ \alpha_eE_s^*+(1-(g+k+n))\alpha_sI_s^*+(1-h)\alpha_fI_f^*-\lambda_2^{**}T^*-\mu T^*=0, \end{cases} \tag{19}$$

where,

$\lambda_1^{**}=\frac{(1-a)(\beta_sI_s^*+\beta_fI_f^*)}{N^*}$, $\lambda_2^{**}=\frac{m\varepsilon(\beta_iI_s^*+\beta_iI_f^*)}{N^*}$ and

$$N^*=S^*+V^*+E_s^*+I_s^*+E_s^*+I_s^*+T^*. \tag{20}$$

Simplifying Eq. (19) gives the following;

$$\begin{cases} S^* = \frac{\left(z_1+\vartheta\lambda_1^{**}\right)((1-b)+\varphi b)\Lambda}{(z_1+\vartheta\lambda_1^{**})(\mu+\lambda_1^{**})}, \\ V^* = \frac{\Lambda b}{z_1+\vartheta\lambda_1^{**}}, \\ E_s^* = \frac{I_s^*}{z_2}\left(y_2 + g\alpha_s + \frac{m\varepsilon\beta_t}{N^*}\left(\frac{(y_2+(g+k+n))\alpha_s)\alpha_e I_s^* + (1-h))\alpha_f I_f^*}{\mu+\lambda_2^{**}}\right)\right), \\ I_s^* = \frac{z_5 - y_8(y_6+\delta_s(y_2+g\alpha_s+y_5)}{\frac{(1-m)\varepsilon\beta_t\alpha_f}{N^*}(y_7 y_8 + n\alpha_s)}, \\ E_f^* = \frac{I_f^*}{z_4}\left(\frac{m\varepsilon\beta_t I_f^* y_3}{N^*} + y_4 + k\alpha_s I_s^* + h\alpha_f\right), \\ I_f^* = \frac{y_6 + y_7 I_s^* + \delta_s(y_2+g\alpha_s+y_5) - z_3}{\frac{(1-m)\varepsilon\beta_t\alpha_f}{N^*}}, \\ T^* = \frac{(y_2+(g+k+n))\alpha_s)\alpha_e I_s^* + (1-h))\alpha_f I_f^*}{\mu+\lambda_2^{**}}. \end{cases} \tag{21}$$

To establish the endemic equilibria, we consider the properties below by defining the invasion reproduction number. The invasion reproduction number described here represents the number of secondary infections that would be generated when the individuals in the drug-sensitive (DS) strain move into the drug-resistant (DR) strain. This is given as

$$R_f^s = \mathcal{P}\left(\check{F}\check{V}^{-1}\right) = \frac{\left(S_f^* + \vartheta V_f^* + \varepsilon T_f^*\right)R_f}{(1-b)(1-\varepsilon)N_f^*}. \tag{22}$$

where $N_f^* = S_f^* + V_f^* + E_f^* + I_f^* + T_f^*$. This represents the total number of individuals belonging to the fast latent class infectious with drug-resistant (DR) strain of TB.

Biologically, at drug-resistant (DR) strain dominance equilibrium, an infectious drug-sensitive (DS) strain will produce R_f^s new infections on the average at any given time. This estimates the power of drug-sensitive (DS) strain moving into the drug-resistant (DR) strain. According to the explanation in (Van den Driessche and Watmough 2002), if $R_f^s < 1$ then D_f^* which denotes the dominance equilibrium of drug-resistant (DR) strain is locally asymptotically stable.

Theorem 3 *If D_f^* exists and $R_f^s < 1$ then the disease-free equilibrium D_f^* is locally asymptotically stable. This signifies that, the drug-resistant (DR) strain infectious individuals approach a limit where the disease becomes endemic if the power of drug-sensitive (DS) strain to invade the system is weak.*

Proof Let's consider new infection matrix representing the drug-resistant (DR) strain equilibrium dominance as follows.

$$\check{F} = \begin{pmatrix} 0 & \frac{(1-a)\beta_s\left[S_f^* + \vartheta V_f^* + \varepsilon T_f^*\right]}{N_s^*} \\ 0 & \frac{a\beta_s\left[S_f^* + \vartheta V_f^* + \varepsilon T_f^*\right]}{N_s^*} \end{pmatrix}, \check{V} = \begin{pmatrix} z_2 & -g\alpha_s \\ -\delta_s & z_3 \end{pmatrix}. \tag{23}$$

Let's consider the following,

$$\rho_a = \left\{\left(S, V, E_s, I_s, E_f, I_f, T\right) | E_s = I_s = E_f = I_f = 0, \; 0 < S \le \frac{\Lambda(1-b)}{\mu}, 0 < V \le \frac{\Lambda b}{\mu}, 0 < T \le \frac{\Lambda}{\mu}\right\}, \tag{24}$$

$$\rho_b = \left\{\left(S, V, E_s, I_s, E_f, I_f, T\right) | E_s = I_s = 0, 0 < S \le \frac{\Lambda(1-b)}{\mu}, \; 0 < V \le \frac{\Lambda b}{\mu}, 0 < E_f \le \frac{\Lambda}{\mu}, 0 < I_f \le \frac{\Lambda}{\mu}, 0 < T \le \frac{\Lambda}{\mu}\right\}, \tag{25}$$

$$\rho_c = \left\{\left(S, V, E_s, I_s, E_f, I_f, T\right) | \begin{matrix} 0 < S \le \frac{\Lambda(1-b)}{\mu}, 0 < V \le \frac{\Lambda b}{\mu}, 0 < E_s \le \frac{\Lambda}{\mu}, 0 < I_s \\ \le \frac{\Lambda}{\mu}, 0 < E_f \le \frac{\Lambda}{\mu}, 0 < I_f \le \frac{\Lambda}{\mu}, 0 < T \le \frac{\Lambda}{\mu} \end{matrix}\right\}. \tag{26}$$

Theorem 4 *If $d_i = 0, i = 1, 2$ and $\varepsilon = 0$, then the dominance equilibrium of drug-resistant (DR) strain is globally asymptotically stable in ρ_b.*

Proof Suppose the following function $\check{D}$ as follows,

$$\check{D} = S - S_f^* - S_f^* lnS + V - V_f^* - V_f^* lnV + E_f - E_f^* lnE_f + \frac{\beta_f\left(S_f^* + V_f^*\right)}{(\mu+\alpha_f)N_f^*}\left(I_f - I_f^* lnI_f\right). \tag{27}$$

The derivative of $\check{D}$ along system (2) is given as,

$$\check{D}'\Big|_f(t) = \left(1 - \frac{S_f^*}{S}\right)S' + \left(1 - \frac{V_f^*}{V}\right)V' + \left(1 - \frac{E_f^*}{E_f}\right)E_f' + \frac{\beta_f\left(S_f^* + V_f^*\right)}{\left(\mu+\alpha_f\right)N_f^*}\left(1 - \frac{I_f^*}{I_f}\right)I_f', \tag{28}$$

$$\begin{aligned} \check{D}'\Big|_f(t) = {} & \left(1 - \frac{S_f^*}{S}\right)\left((1-b)\Lambda + \varphi V - \frac{\beta_f I_f S}{N} - \mu S\right) \\ & + \left(1 - \frac{V_f^*}{V}\right)\left(b\Lambda - \frac{\beta_f I_f \vartheta V}{N} - (\mu+\varphi)V\right) \\ & + \left(1 - \frac{E_f^*}{E_f}\right)\left(\frac{(1-a)\beta_f I_f[S+\vartheta V] + m\varepsilon\beta_t T I_f}{N} + h\alpha_f I_f - (\mu+\delta_f)E_f\right) \\ & + \frac{\beta_f\left(S_f^* + V_f^*\right)}{(\mu+\alpha_f)N_f^*}\left(1 - \frac{I_f^*}{I_f}\right) \\ & \left(\frac{a\beta_f I_f[S+\vartheta V] + (1-m)\varepsilon\beta_t T I_f}{N} + \delta_f E_f - (\mu+\alpha_f)E_f\right). \end{aligned} \tag{29}$$

$d_i = 0, i = 1,2$ and $\varepsilon = 0$, then $N_f^* = N$.

$$\check{D}\prime\Big|_f(t) = \mu S_f^*\left(2 - \frac{S_f^*}{S} - \frac{S}{S_f^*}\right) + \mu V_f^*\left(2 - \frac{V_f^*}{V} - \frac{V}{V_f^*}\right) + \frac{\beta_f S_f^* I_f^*}{N_f^*}\left(3 - \frac{S_f^*}{S} - \frac{SE_f^* I_f}{S_f^* E_f I_f^*} - \frac{E_f I_f^*}{E_f^* I_f}\right) + \frac{\beta_f V_f^* I_f^*}{N_f^*}\left(3 - \frac{V_f^*}{\vartheta V} - \frac{\vartheta V E_f^* I_f}{V_f^* E_f I_f^*} - \frac{E_f I_f^*}{E_f^* I_f}\right). \tag{30}$$

Since the arithmetic mean of any positive numbers is greater than or equal to their geometric mean, it follows that $\check{D} \leq 0.\check{D} = 0$ only holds if $S = S_f^*, V = V_f^*, E_f = E_f^*, I_f = I_f^*$. According to the Lyapunov-LaSalle stability theorem analysis, the solution of system (2) has drug-resistant strain equilibrium dominance.

Theorem 5 *Suppose that* $R_s > 1, R_f > 1$ *and* $R_f^s > 1$, *it is obvious that system (2) is insistently repetitive, then there is* $\sigma > 0$ *and*;

$$\liminf_{t\to\infty} I_j^*(t) > \sigma, j = s, f. \tag{31}$$

Proof If the disease-free equilibrium D_f^* is globally asymptotically stable, then based on Theorem 3 above, ρ_a is ejective to ρ_c whenever $R_s > 1$ and $R_f > 1$. Therefore, the drug-resistant (DR) equilibrium is globally asymptotically stable and ρ_b is ejective to ρ_c when $R_f^s > 1$. It follows that limit set $\rho(\partial\rho_c) = \{D_0, D_f\}$ as explained in (Hale and Waltman 1981). Therefore, there exists an insistent repetitive system.

Numerical scheme

Estimation of model parameters and partial rank correlation coefficient (PRCC)

In this section, we evaluate the parameters in model (2), evaluate the reproduction numbers R_s and R_f, evaluate the sensitivity index of the parameters and explore their relation with the reproduction numbers. We also show the graphical representation of the results to analyze the transmission dynamics of TB. The parameters values are tabulated in Table 1. The figure below illustrates the cumulative TB cases recorded within 22 years (2000–2022) in Ghana by the World Health Organization (WHO 2023).

Now, we investigate relationship between the parameters and I_s, I_f by considering the behavioral patterns of the respective parameters associated with slow latent class and fast latent class on the reproduction numbers R_s, R_f the graphical representations are illustrated below. Once the model fits the actual data (see Fig. 2a), we evaluate the effective reproduction number $R_e = \mathcal{P}(FV^{-1}) = \max\{R_s, R_f\}$ as follows. The reproduction number of the slow latent class infectious with drug-sensitivity (DS) strain of TB, $R_s = 0.27$. The reproduction number of the fast latent class infectious with drug-resistant (DR) strain of TB, $R_f = 2.23$. It is obvious that the drug-resistant (DR) strain of TB is dominant in the population, therefore the effective reproduction number $R_e = 2.23$. The effective reproduction number indicates that one infectious TB patient will generate two secondary infections at any given time when he/she come into contact with people living in safe zone. This calls for the extra interventions to control the transmission of the disease.

Figure 2b shows the partial rank correlation coefficients (PRCC) of the parameters associated with R_s which depicts

Table 1 Definition of model parameters and values

Parameter	Definition	Value	Reference
β_s	Effective contact rate of slow latent class	0.3	Gomes et al. (2004)
β_f	Effective contact rate of fast latent	0.5	Dontwi et al. (2014)
β_t	Effective contact rate of treated individuals	0.2	Trauer et al. (2014)
ϑ	Rate of vaccines protection	0.5	Fitted
φ	Waning rate of immunity	0.05	Mettle et al. (2020)
δ_s	Incubation period of the slow latent class	0.14	Dontwi et al. (2014)
δ_f	Incubation period of fast latent class	0.34	Dontwi et al. (2014)
E	Movement from $T(t)$ due to treatment failure	0.25	Fitted
Λ	Rate of recruitment	1364	Estimated
μ	Rate of natural death	0.000043	Estimated
α_s	Treatment rate of slow latent class	0.2	Trauer et al. (2014)
α_f	Treatment rate of fast latent class	0.01	Fitted
α_e	Treatment rate of $E_s(t)$ individuals	0.1	Fitted
d_i	Death induced by tuberculosis	0.000017	Dontwi et al. (2014)

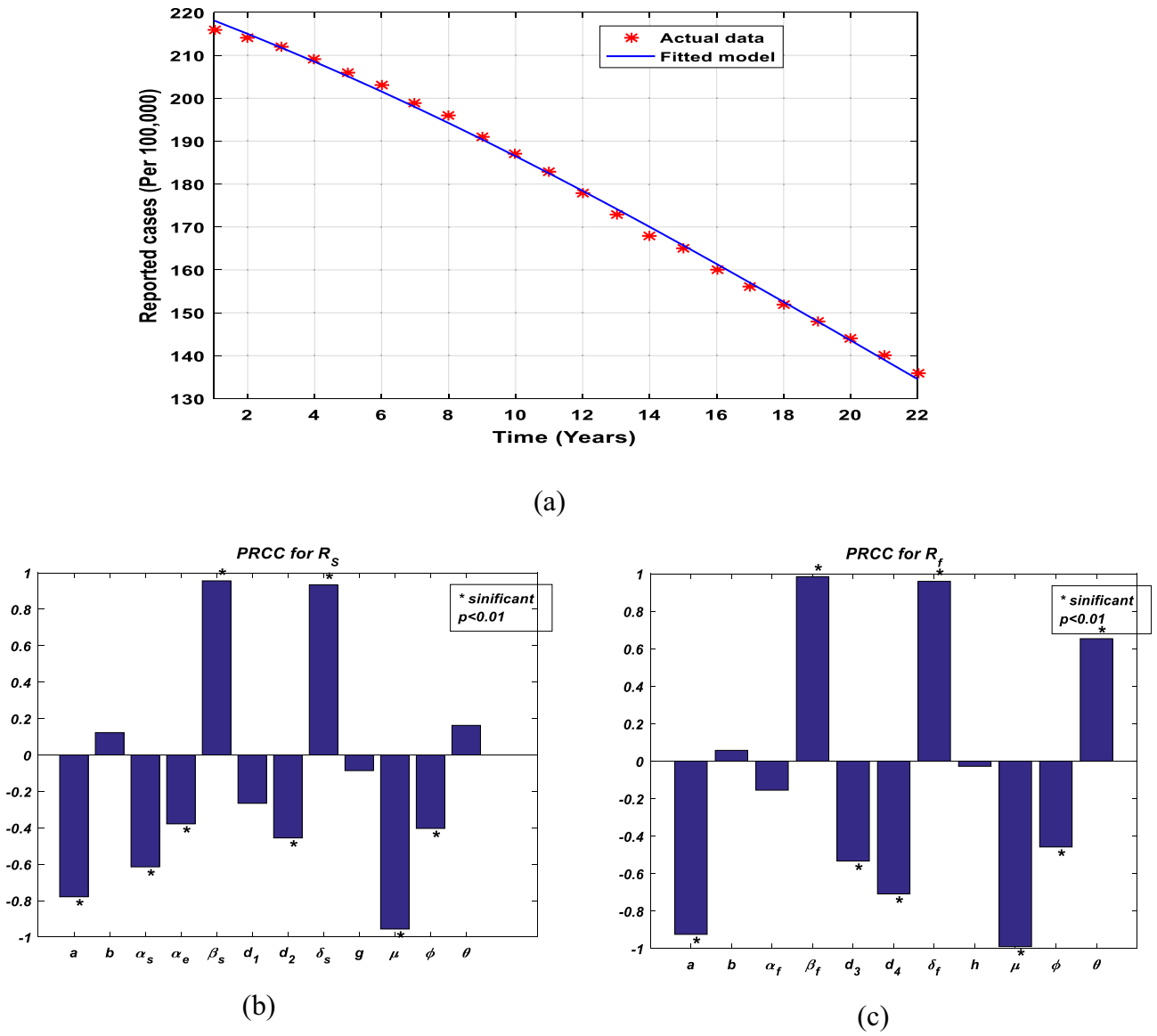

Fig. 2 **a** Cumulative Tuberculosis (TB) reported cases from the year 2000 to 2022, **b** and **c** show the partial rank correlation (PRCC) of the parameters in R_s andR_f

the transmission dynamics of the slow latent class infectious with drug-sensitive (DS) strain of TB. It is observed that (β_s, δ_s) have a high positive effect on the reproduction number R_s and $(a, \alpha_s, \alpha_e, \varphi, \mu, d_2)$ have a negative impact on the reproduction number R_s. Figure 2c shows the partial rank correlation coefficients (PRCC) of the parameters associated with R_f which depicts the transmission dynamics of the fast latent class infectious with DR strain of TB. It is observed that $(\beta_f, \delta_f, \vartheta)$ have a high positive impact on the reproduction number R_f and $(a, \varphi, \mu, d_3, d_4)$ have a negative impact on the reproduction number R_f. This is determined by the associated sign, those with the positive sign indicates a perfect relationship and the negative sign indicates an imperfect relationship. If the value is high then there exist a strong relationship and the lower the value, the weaker the relation between the input and the output value. Also, it is noticed that in all the classes, the vaccination protection rate ϑ increases the reproduction number therefore there should be measures to optimally control the spread of tuberculosis.

In order to formulate control strategies to minimize the spread of TB, we demonstrate the transmission dynamics in different scenarios in the figures below based on the parameters that exhibit strong relationship with the reproduction numbers as demonstrated in Fig. 3.

Figure 3a and b represent the respective contour plots of the reproduction numbers R_s and R_f as a function of effective contact rates and the incubation periods of the two latent classes. The two figures imply that to significantly

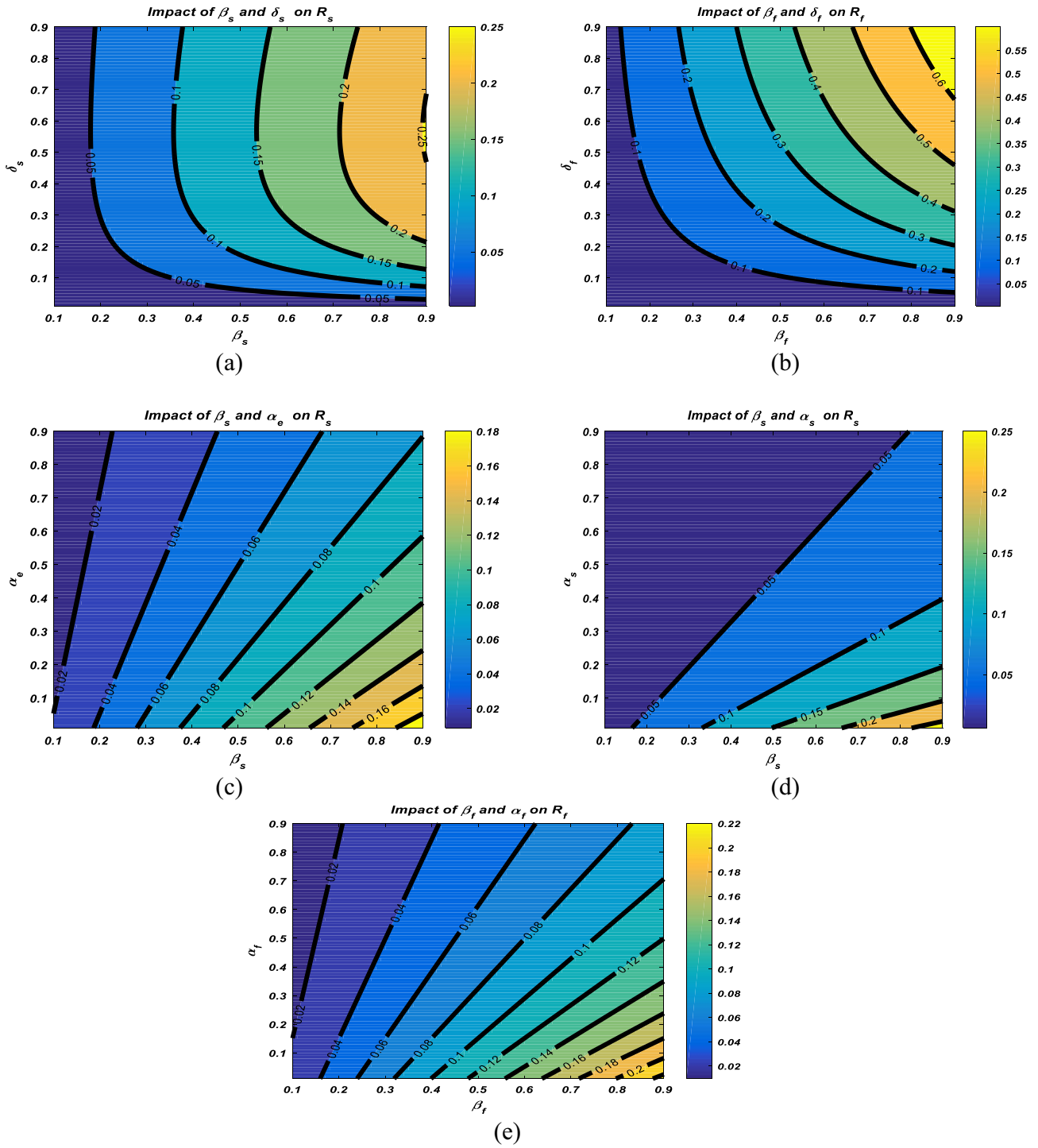

Fig. 3 **a**, **b** Show the relationship between the effective contact rate of DS strain β_s, DR strain β_f and their respective incubation period, **c–e** show the relationship between the effective contact rate of DS strain β_s, DR strain β_f and their respective treatment rate, **f–i** show the relationship between the effective contact rate of DS strain β_s, DR strain β_f and vaccination

reduce the basic reproduction number to a minimum requires measures that are non-pharmaceutical such as the mask usage and social distancing etc., to reduce the effective contact rate to prolong the period of acquiring the disease which reduces the incubation rates.

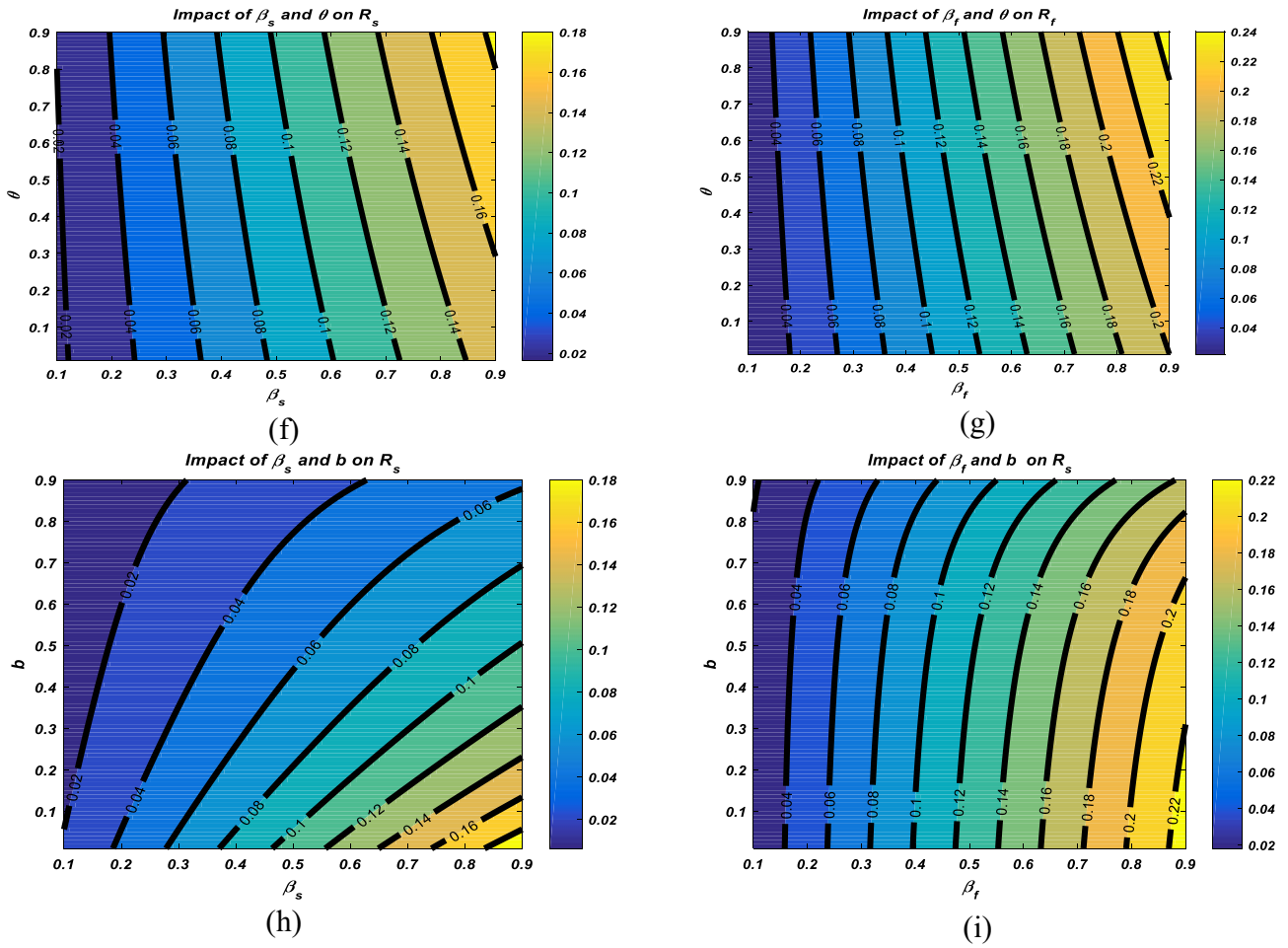

Fig. 3 (continued)

Figure 3c–e show the respective contour plots of the reproduction numbers R_s and R_f as a function of effective contact rates and the treatment rates of the two latent classes. The three figures imply that to significantly reduce the basic reproduction number to a minimum requires both pharmaceutical measures such as effective prophylaxis and non-pharmaceutical measures such as the mask usage and social distancing etc., to reduce the effective contact rate and improve the treatment rates of the two latent classes.

Figure 3f and g show the respective contour plots of the reproduction numbers R_s and R_f as a function of effective contact rates and the vaccines protection rate. Figure 3h and i show the respective contour plots of the reproduction numbers R_s and R_f as a function of effective contact rates and the vaccination coverage of newborns of the two latent classes. The figures imply that to significantly reduce the basic reproduction number to a minimum requires both pharmaceutical measures such as effective prophylaxis and non-pharmaceutical measures such as the mask usage and social distancing etc., to reduce the effective contact rate and intensify vaccination.

All the above illustrations depict the dynamics of the PRCC plots in Fig. 2b and c. It is realized that all these parameters have either positive or negative effect on the transmission of the tuberculosis. In order to reduce spread, then there must be effective control efforts to reduce the rate of secondary infections thus R_s and R_f of the two latent classes.

Optimal control analysis

We modify model (2) with the optimal control the following control variables $U_p(t)$, as the public education on the prevention of TB such as mask usage, social distancing where $U_p(t) \in [0,1]$, which reduces the force of infection, λ_1 by $1 - U_p(t).U_v(t)$; control effort to intensify vaccination of newborns by $1 + U_v(t).U_s(t)$; control effort to enhance prophylaxis of the individuals in the slow latent class by

$1 + U_s(t)$ hence those identified to be infectious will be go through prophylaxis in order to halt the infections that may occur. The control effort $U_f(t)$ is control for treatment failure in the slow latent class in order to minimize the occurrence of drug-resistant strain of TB by $1 - U_f(t)$. All these efforts denote the admissible control measures necessary to minimize the transmission of the disease.

Through Pontryagin's maximum principle, system (31) and the objective functional (32) are transformed into a state of point wise Hamiltonian H. The following optimal solution is achieved.

$$\begin{cases} \frac{dS}{dt} = \left[1-(1+U_v)b\right]\Lambda + \varphi V - \left[\left(1-U_p\right)\lambda - \mu\right]S, \\ \frac{dV}{dt} = \left(1+U_v\right)b\Lambda - \left[\left(1-U_p\right)\lambda\vartheta - (\mu+\varphi)\right]V, \\ \frac{dE_s}{dt} = \left(1-U_p\right)\omega_1[S+\vartheta V] + \omega_6 T + \left[1-U_f(t)\right]g\alpha_s I_s - \left(\mu + d_1 + \delta_s + \left(1+U_s\right)\alpha_e\right)E_s, \\ \frac{dI_s}{dt} = \left(1-U_p\right)\omega_2[S+\vartheta V] + \omega_5 T + \delta_s E_s - \left(\mu + d_2 + \left(1-U_f\right)\alpha_s\right)I_s, \\ \frac{dE_f}{dt} = \left(1-U_p\right)\omega_3[S+\vartheta V] + \omega_8 T + \left[1-U_f\right]k\alpha_s I_s + h\alpha_f I_f - \left(\mu + d_3 + \delta_f\right)E_f, \\ \frac{dI_f}{dt} = \left(1-U_p\right)\omega_4[S+\vartheta V] + \omega_7 T + \left[1-U_f\right]n\alpha_s I_s + \delta_f E_f - \left(\mu + d_4 + h\alpha_f\right)I_f, \\ \frac{dT}{dt} = \left(1+U_s\right)\alpha_e E_s + \left[1-U_f\right]\left[(1-(g+k+n))\alpha_s I_s\right] + (1-h)\alpha_f I_f - (\mu+\varepsilon\lambda)T. \end{cases} \tag{31}$$

where $\lambda = \frac{(1-a)(\beta_s I_s + \beta_f I_f)}{N}, \omega_1 = \frac{(1-a)\beta_s I_s}{N}, \omega_2 = \frac{a\beta_s I_s}{N}, \omega_3 = \frac{(1-a)\beta_f I_f}{N}, \omega_4 = \frac{a\beta_f I_f}{N}, \omega_5 = \frac{(1-m)\varepsilon\beta_s I_s}{N}, \omega_6 = \frac{m\varepsilon\beta_s I_s}{N}, \omega_7 = \frac{(1-m)\varepsilon\beta_f I_f}{N}, \omega_8 = \frac{m\varepsilon\beta_f I_f}{N}$. With initial conditions $S(0) \geq 0$ $V(0) \geq 0, E_s(0) \geq 0, I_s(0) \geq 0, E_f(0) \geq 0, I_f(0) \geq 0, T(0) \geq 0$.

Objective functional

We now formulate the optimal trajectories that show the effect of the control efforts $U_p(t), U_v(t), U_s(t)$ and $U_f(t)$ subjected to (16). The objective functional B is given as,

$$B(U_p, U_v, U_s, U_f) = \int_0^{t_f} \left[b_1 E_s + b_2 I_s + b_3 E_f + b_4 I_f + \frac{1}{2}C_p U_p^2(t) + \frac{1}{2}C_v U_v^2(t) + \frac{1}{2}C_s U_s^2(t) + \frac{1}{2}C_f U_f^2(t)\right]dt. \tag{32}$$

We focus on minimizing the cost function (32), the total cost of implementing the optimal control is given as;

$$M = \int_0^{t_f} \left[\frac{1}{2}C_p U_p^2(t) + \frac{1}{2}C_v U_v^2(t) + \frac{1}{2}C_s U_s^2(t) + \frac{1}{2}C_f U_f^2(t)\right]dt. \tag{33}$$

The parameters c_1, c_2, c_3 and c_4 are the balancing cost factors for $U_p(t), U_v(t), U_s(t), U_f(t)$ respectively. All the control efforts $U_p(t), U_v(t), U_s(t), U_f(t)$ are assumed to be bounded by Lebesgue measurable time-dependent functions on the interval $[0, t_f]$, where t_f is the final time with the control effort set defined as;

$$\Gamma = \left(U_p(t), U_v(t), U_s(t), U_f(t)(t)\right) \text{ for} \left(0 \leq U_p(t), U_v(t), U_s(t), U_f(t) \leq 1, \right), 0 \leq t \leq t_f\big). \tag{34}$$

$$\begin{aligned} H =& b_1 E_s + b_2 I_s + b_3 E_f + b_4 I_f + \frac{1}{2}C_p U_p^2(t) + \frac{1}{2}C_v U_v^2(t) \\ &+ \frac{1}{2}C_s U_s^2(t) + \frac{1}{2}C_f U_f^2(t) \\ &+ \lambda_S\left(\left[1-(1+U_v)b\right]\Lambda + \varphi V - \left[\left(1-U_p\right)\lambda - \mu\right]S\right) \\ &+ \lambda_V\left(\left(1+U_v\right)b\Lambda - \left[\left(1-U_p\right)\lambda\vartheta - (\mu+\varphi)\right]V\right) \\ &+ \lambda_{E_s}\left(\left(1-U_p\right)\omega_1[S+\vartheta V] + \omega_5 T + \left[1-U_f\right]g\alpha_s I_s\right. \\ &\left.-\left(\mu + d_1 + \delta_s + \left(1+U_s\right)\alpha_e\right)E_s\right) \\ &+ \lambda_{I_s}\left(\left(1-U_p\right)\omega_2[S+\vartheta V] + \omega_6 T + \delta_s E_s\right. \\ &\left.-\left(\mu + d_2 + \left(1-U_f\right)\alpha_s\right)I_s\right) \\ &+ \lambda_{E_f}\left(\left(1-U_p\right)\omega_3[S+\vartheta V] + \omega_7 T\right. \\ &\left.+\left[1-U_f\right]k\alpha_s I_s + h\alpha_f I_f - \left(\mu + d_3 + \delta_f\right)E_f\right) \\ &+ \lambda_{I_f}\left(\left(1-U_p\right)\omega_4[S+\vartheta V] + \omega_8 T\right. \\ &\left.+\left[1-U_f\right]n\alpha_s I_s + \delta_f E_f - \left(\mu + d_4 + h\alpha_f\right)I_f\right) \\ &+ \lambda_T\left(\left(1+U_s\right)\alpha_e E_s + \left[1-U_f\right]\right. \\ &\left.\left[(1-(g+k+n))\alpha_s I_s\right] + (1-h)\alpha_f I_f - (\mu+\varepsilon\lambda)T\right). \end{aligned} \tag{35}$$

where $\lambda_S, \lambda_V, \lambda_{E_s}, \lambda_{I_s}, \lambda_{E_f}, \lambda_{I_f}, \lambda_T$ are the costate variables with respect to the state variables, $S, V, E_s, I_s, E_f, I_f, T$.

Theorem 6 *Given $U_p^*(t), U_v^*(t), U_s^*(t), U_f^*(t)$ as the optimal controls and the corresponding solutions $S^0, V^0, E_s^0, I_s^0, E_f^0, I_f^0, T^0$ of system (35) which minimizes $M\left(U_p(t), U_v(t), U_s(t), U_f(t)\right)$ over Γ, then there exist costate variables $\lambda_S, \lambda_V, \lambda_{E_s}, \lambda_{I_s}, \lambda_{E_f}, \lambda_{I_f}, \lambda_T$ that satisfy*

$$\frac{d\lambda_j}{dt} = -\frac{\partial H}{\partial j}. \tag{36}$$

With conditions; $\lambda_j(t_f) = 0$, where $j = S, V, E_s, I_s, E_f, I_f, T$. Then the optimality conditions that minimize the

Hamiltonian, H of (35) with respect to the controls are given as;

We solve for $U_p(t), U_v(t), U_s(t)$ and $U_f(t)$ as $U_p^*(t), U_v^*(t), U_s^*(t)$ and $U_f^*(t)$

$$\begin{cases} U_p^*(t) = \min\left\{ U_p\max,\ \max\left(0, \frac{(S^0+\vartheta V^0)\left(\omega_1\lambda_{E_s}+\omega_2\lambda_{I_s}+\omega_3\lambda_{E_f}+\omega_4\lambda_{I_f}\right)-\lambda\left(\lambda_S S^0+\lambda_V\vartheta V^0\right)}{C_p} \right) \right\}, \\ U_v^*(t) = \min\left\{ U_v\max,\ \max\left(0, \frac{(\lambda_S-\lambda_V)b\Lambda}{C_v} \right) \right\}, \\ U_s^*(t) = \min\left\{ U_s\max,\ \max\left(0, \frac{(\lambda_{E_s}-\lambda_T)\alpha_e E_s^0}{C_s} \right) \right\}, \\ U_f^*(t) = \min\left\{ U_f\max,\ \max\left(0, \frac{\left((\lambda_{E_s}-\lambda_T)g+\left(\lambda_{E_f}-\lambda_T\right)k+\left(\lambda_{I_f}-\lambda_T\right)n+\lambda_T\right)\alpha_s I_s^0}{C_f} \right) \right\}. \end{cases} \tag{37}$$

Proof We take the partial derivative of Eq. (35) with respect to the solutions of the system, optimal control and final time conditions. The adjoint equation is demonstrated below.

of Eq. (39) and the results are as follows,

$$\begin{cases} \frac{d\lambda_S}{dS} = [1-U_p]\left[(\lambda_{E_s}-\lambda_S)\omega_1+(\lambda_{I_s}-\lambda_S)\omega_2+\left(\lambda_{E_f}-\lambda_S\right)\omega_3+\left(\lambda_{I_f}-\lambda_S\right)\omega_4\right]+(\lambda_S-\lambda_V)\varphi V+\mu\lambda_S, \\ \frac{d\lambda_V}{dV} = [1-U_p]\vartheta\left[(\lambda_{E_s}-\lambda_V)\omega_1+(\lambda_{I_s}-\lambda_V)\omega_2+\left(\lambda_{E_f}-\lambda_V\right)\omega_3+\left(\lambda_{I_f}-\lambda_V\right)\omega_4\right]+(\lambda_S-\lambda_V)\varphi+\mu\lambda_V, \\ \frac{d\lambda_{E_s}}{dE_s} = -b_1+[1-U_p]\omega_1\left[(\lambda_{E_s}-\lambda_S)S+(\lambda_{E_s}-\lambda_V)\vartheta V\right]+(\lambda_{E_s}-\lambda_{I_s})(1-U_f)g\alpha_s+(\lambda_{E_s}-\lambda_T)\omega_6 T+ \\ (\lambda_{I_s}-\lambda_{E_s})\delta_s+(\lambda_T-\lambda_{E_s})(1+U_s)\alpha_e+(\mu+d_1)\lambda_{E_s}, \\ \frac{d\lambda_{I_s}}{dI_s} = -b_2+[1-U_p]\omega_2\left[(\lambda_{E_s}-\lambda_S)S+(\lambda_{E_s}-\lambda_V)\vartheta V\right]+(\lambda_{I_s}-\lambda_{E_s})\delta_s E_s+(\lambda_{I_s}-\lambda_T)\omega_5 T+\left(\lambda_{I_f}-\lambda_{I_s}\right)(1-U_f)n\alpha_s \\ +[1-U_f]\left[(\lambda_{E_s}-\lambda_{I_s})g+\left(\lambda_{E_f}-\lambda_{I_s}\right)k\right]\alpha_s+(\lambda_T-\lambda_{I_s})(1-U_f)(1-(g+k+n))\alpha_s+(\mu+d_2)\lambda_{I_s}, \\ \frac{d\lambda_{E_f}}{dE_f} = -b_3+[1-U_p]\omega_3\left[\left(\lambda_{E_f}-\lambda_S\right)S+\left(\lambda_{E_f}-\lambda_V\right)\vartheta V\right]+\left(\lambda_{E_f}-\lambda_T\right)\omega_8 T+\left(\lambda_{E_f}-\lambda_{I_s}\right)(1-U_f)k\alpha_s I_s+ \\ \left(\lambda_{E_f}-\lambda_{I_f}\right)h\alpha_f I_f+\left(\lambda_{E_f}-\lambda_{I_f}\right)\delta_f+(\mu+d_3)\lambda_{E_f}, \\ \frac{d\lambda_{I_f}}{dI_f} = -b_4+[1-U_p]\omega_4\left[\left(\lambda_{I_f}-\lambda_S\right)S+\left(\lambda_{I_f}-\lambda_V\right)\vartheta V\right]+\left(\lambda_{I_f}-\lambda_{E_f}\right)\delta_f+(\lambda_{I_s}-\lambda_T)\omega_7 T+ \\ \left(\lambda_{I_f}-\lambda_{I_s}\right)(1-U_f)n\alpha_s I_s+\left(\lambda_{E_f}-\lambda_{I_f}\right)(1-h)\alpha_f+(\mu+d_4)\lambda_{I_f}, \\ \frac{d\lambda_T}{dT} = (\lambda_T-\lambda_{E_s})(1+U_s)\alpha_e E_s+[1-U_f]\left[(\lambda_T-\lambda_{I_s})(1-(g+k+n))\alpha_s I_s\right]+(\lambda_T-\lambda_{E_s})(1-h)\alpha_f I_f+ \\ (\lambda_{E_s}-\lambda_T)\omega_6+(\lambda_{I_s}-\lambda_T)\omega_5+\left(\lambda_{E_f}-\lambda_T\right)\omega_8+\left(\lambda_{I_f}-\lambda_T\right)\omega_7+\mu\lambda_T. \end{cases} \tag{38}$$

The control set below illustrates the costate system with the optimal conditions.

$$\begin{cases} \frac{\partial H}{\partial U_p} = C_p U_p+\lambda\left(\lambda_S S^0+\lambda_V\vartheta V^0\right)-\left(S^0+\vartheta V^0\right)\left(\omega_1\lambda_{E_s}+\omega_2\lambda_{I_s}+\omega_3\lambda_{E_f}+\omega_4\lambda_{I_f}\right), \\ \frac{\partial H}{\partial U_v} = C_v U_v+\left(\lambda_V-\lambda_S\right)b\Lambda, \\ U_s^*(t) = \frac{\partial H}{\partial U_s} = C_s U_s+\left(\lambda_T-\lambda_{E_s}\right)\alpha_e E_s^0, \\ \frac{\partial H}{\partial U_f} = C_f U_f-\left(g\lambda_{E_s}+k\lambda_{E_f}+n\lambda_{I_f}\right)\alpha_s I_s^0-(1-(g+k+n))\lambda_T\alpha_s I_s^0. \end{cases} \tag{39}$$

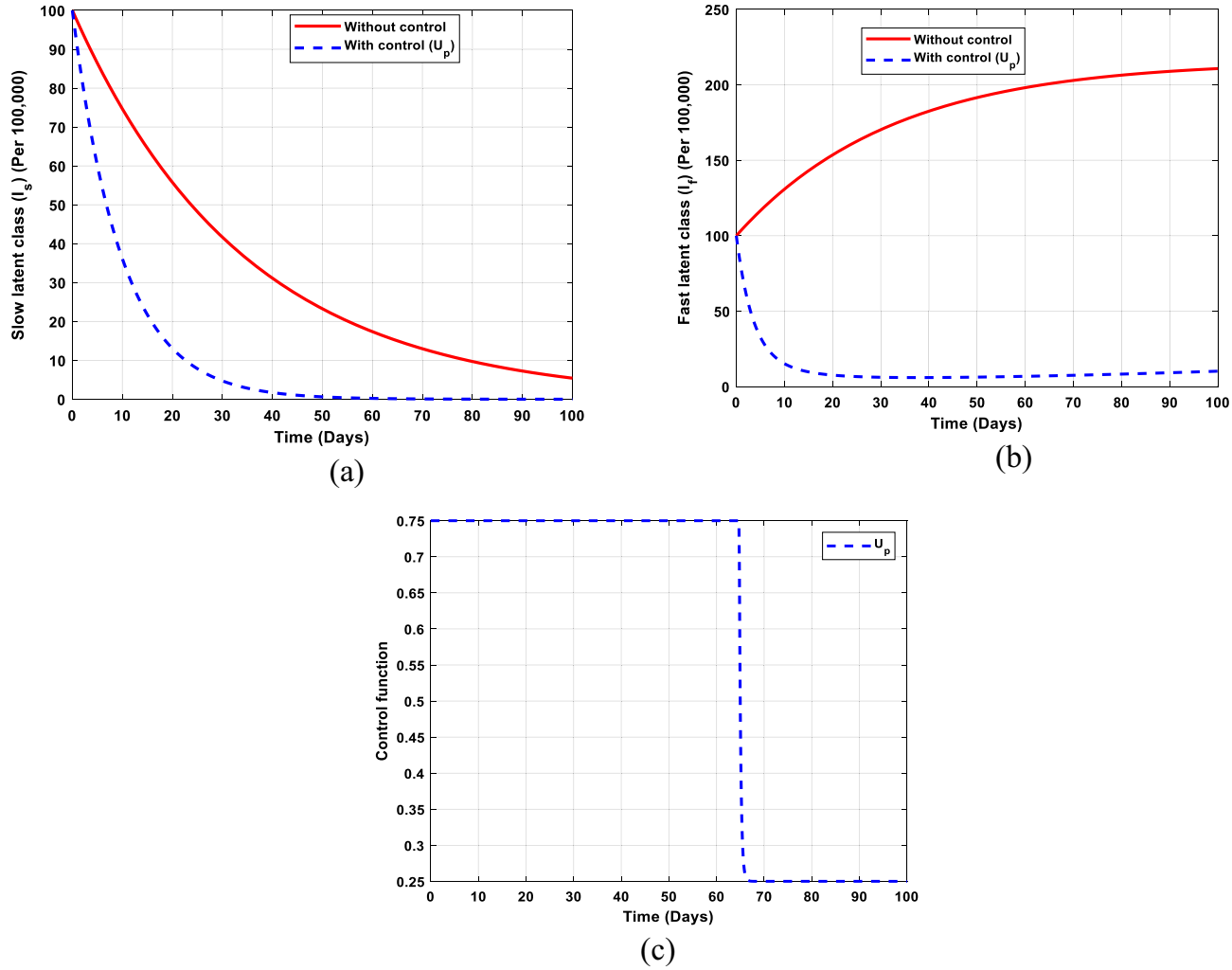

Fig. 4 Optimal solutions of implementing strategy 1

$$\begin{cases} U_p^*(t) = \dfrac{(S^0+\vartheta V^0)\left(\omega_1\lambda_{E_s}+\omega_2\lambda_{I_s}+\omega_3\lambda_{E_f}+\omega_4\lambda_{I_f}\right)-\lambda\left(\lambda_S S^0+\lambda_V\vartheta V^0\right)}{C_p}, \\ U_v^*(t) = \dfrac{(\lambda_S-\lambda_V)b\Lambda}{C_v}, \\ U_s^*(t) = \dfrac{(\lambda_{E_s}-\lambda_T)\alpha_e E_s^0}{C_s}, \\ U_f^*(t) = \dfrac{\left((\lambda_{E_s}-\lambda_T)g+\left(\lambda_{E_f}-\lambda_T\right)k+\left(\lambda_{I_f}-\lambda_T\right)n+\lambda_T\right)\alpha_s I_s^0}{C_f}. \end{cases} \tag{40}$$

Therefore, using the bounds of the controls $U_p^*(t), U_v^*(t), U_s^*(t)$ and $U_f^*(t)$, the control efforts are in the compact form given by the optimal condition of the system; hence the proof is complete.

Results

Results of optimal control

We explore the dynamics of implementing the control efforts, the optimality system (31) is evaluated forward in time and adjoint system (38) backward in time with the corresponding lower and upper bounds of the controls. The estimated total population of Ghana is 31732129 (Osei et al. 2023), hence $N(0) = 31732129$. The initial conditions for the state variables per 100,000 people are as follows; $S(0) = 500, V(0) = 80, E_s(0) = 120, I_s(0) = 100, E_f(0) = 120, I_f(0) = 100 \text{and} T(0) = 50$, together with parameter values illustrated in Table 1. The balance costs associated with the objective functional are assumed as $C_1 = 10, C_2 = 20, C_3 = 30, C_4 = 60$ and weights $b_1 = 1, b_2 = 1, b_3 = 1, b_4 = 1$. The lower bound (LB) and upper bound (UB) are assumed as

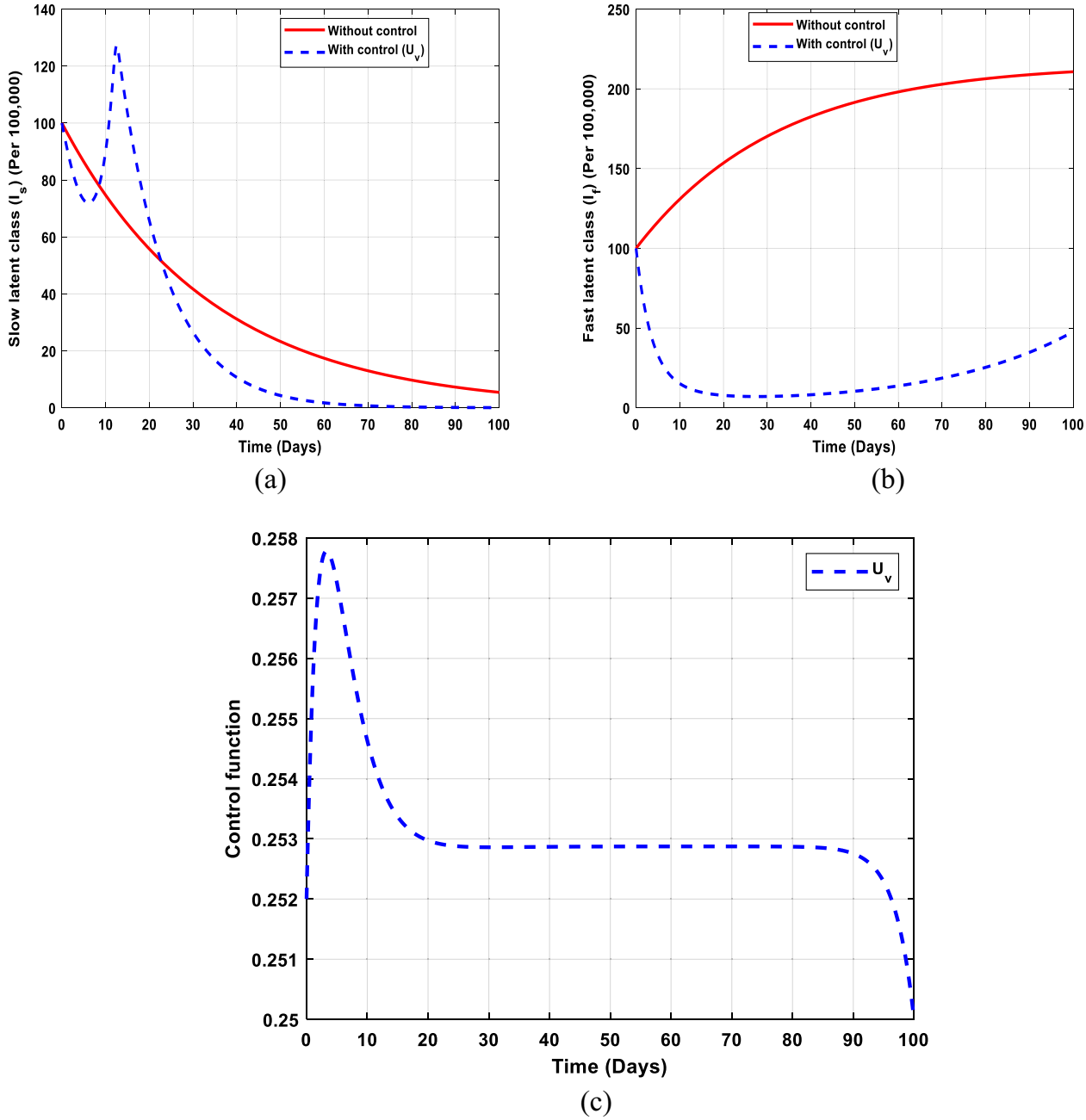

Fig. 5 Optimal solutions of implementing strategy 2

$LB_1 = 0, UB_1 = 1, LB_2 = 0, UB_2 = 1, LB_3 = 0, UB_3 = 1$. The results are illustrated below.

Strategy 1: implementation of public education (U_p)

The optimal solutions illustrated in Fig. 4 accounts the observations when the control effort U_p is applied accordingly.

The optimal solutions illustrated above depict the following observations when public education only is applied.

(a) Figure 4 represents the effect of the control effort U_p on infectious drug sensitive (DS) strain of TB individuals. It implies that, the number of individuals will decrease to the minimum within 40 days if the control effort is optimally implemented in halting the disease's transmission.

(b) Figure 4 represents the effect of the control effort U_p on infectious drug resistant (DR) strain of TB indi-

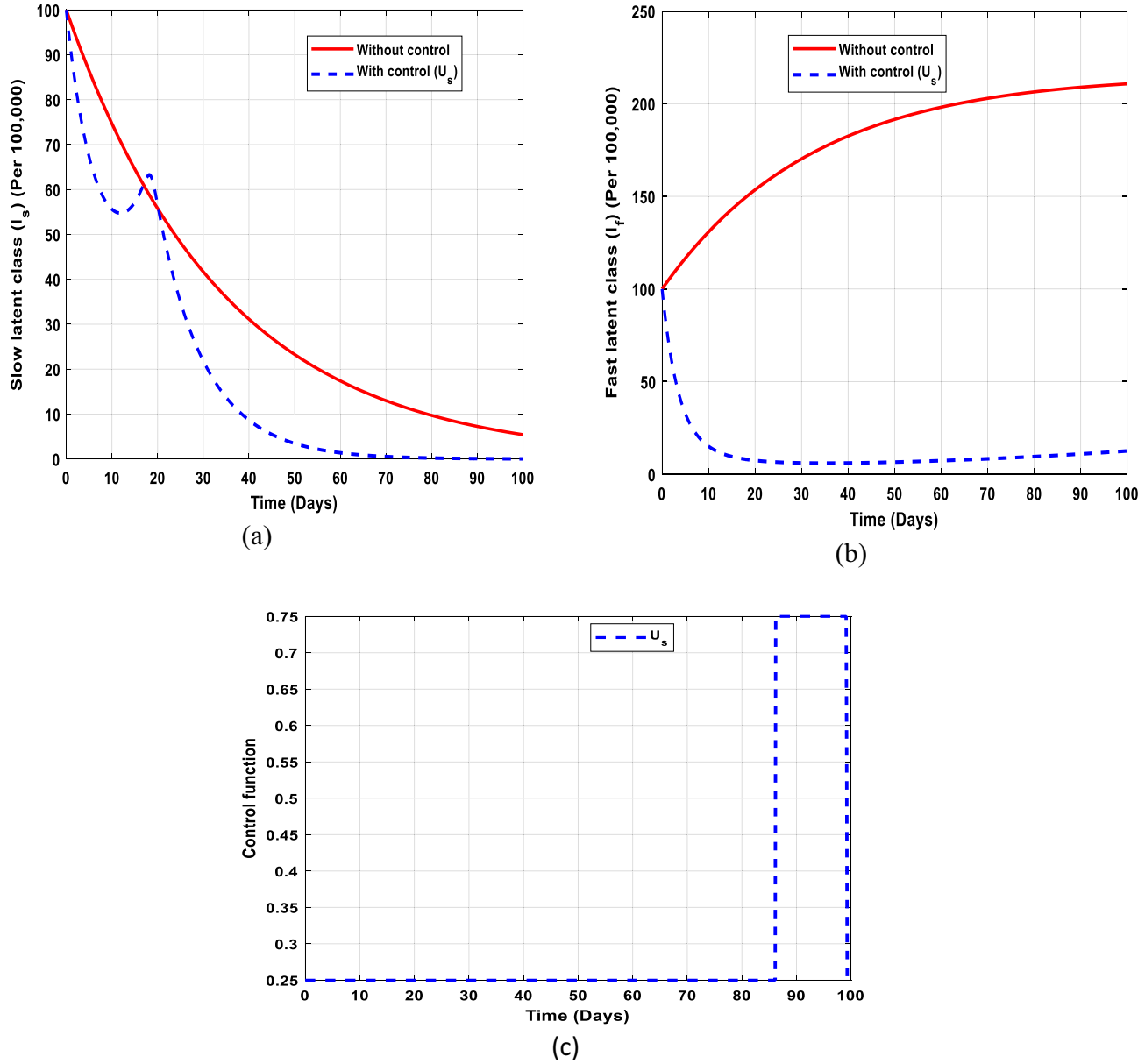

Fig. 6 Optimal solutions of implementing strategy 3

viduals. It implies that, the number of individuals will decrease to the minimum within 50 days if the control effort is optimally implemented in halting the disease's transmission. Conversely, it will increase significantly.

(c) Figure 4 represents the profile of control effort for public education on tuberculosis. It implies that, the education on TB should reach about 75% of the population within 65 days and can be relaxed to about 25% throughout the implementation in minimizing tuberculosis transmission.

Strategy 2: implementation of vaccination (U_v)

The optimal solutions illustrated in Fig. 5 accounts the observations when the control effort U_v is applied accordingly.

The optimal solutions illustrated above depict the following observations when vaccination only is applied.

(a) Figure 5 represents the effect of the control effort U_v on infectious drug sensitive (DS) strain of TB individuals. It implies that, the number of individuals will decrease to the minimum within 65 days if the control effort is optimally implemented in halting the disease's trans-

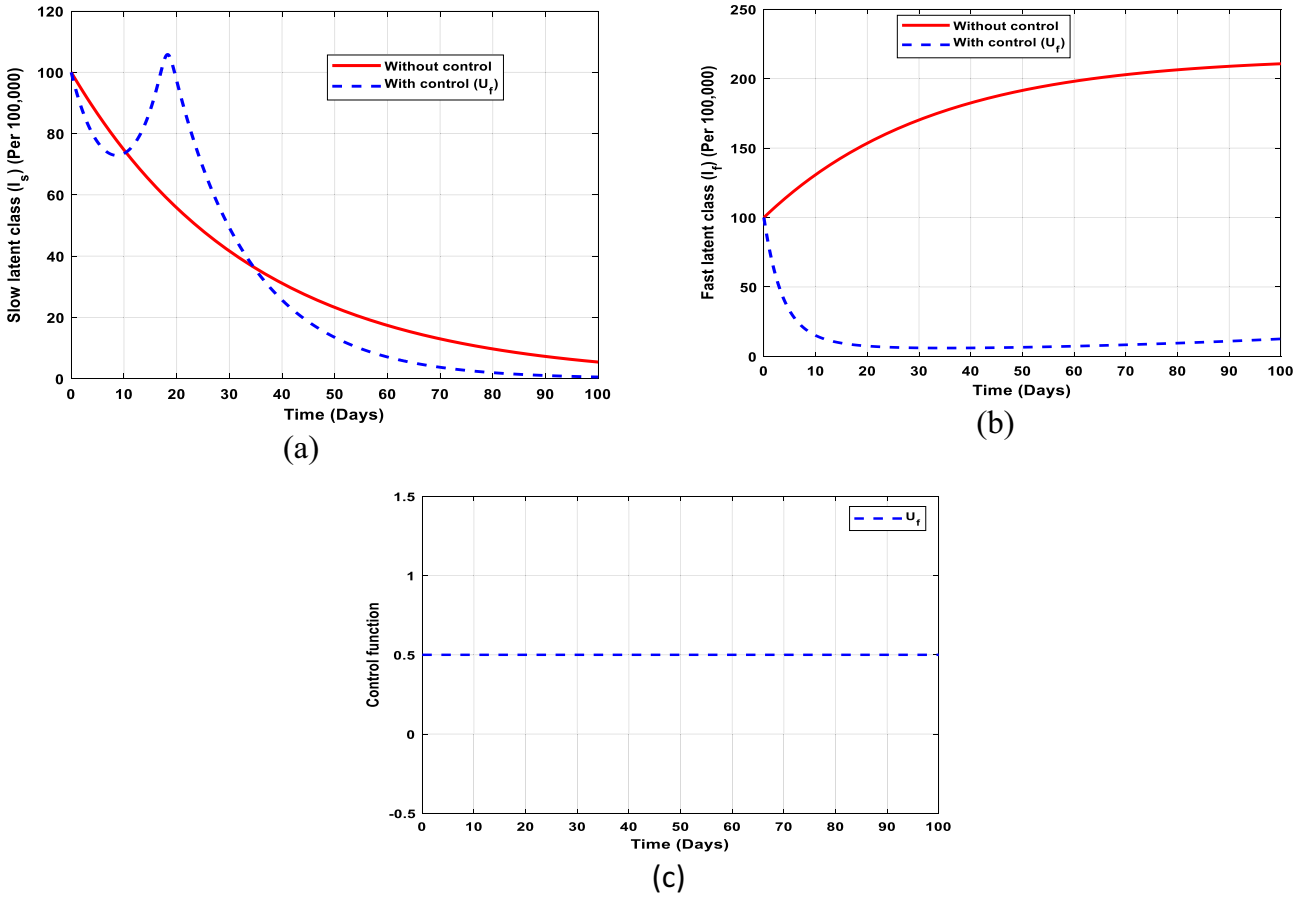

Fig. 7 Optimal solutions of implementing strategy 4

mission. However, it should be done with care because of the ability of drug-resistant strain invasion.

(b) Figure 5 represents the effect of the control effort U_v on infectious drug resistant (DR) strain of TB individuals. It implies that, the number of individuals will decrease if the control effort is optimally implemented in halting the disease's transmission, but will rise at the latter part of implementation. Hence, implementing only this intervention needs extra care.

(c) Figure 5 represents the profile of control effort for tuberculosis vaccination. It implies that, the TB vaccination should be relaxed to about 25% throughout the implementation because of the occurrence of drug-resistant strain of TB.

Strategy 3: implementation of case finding (U_s)

The optimal solutions illustrated in Fig. 6 accounts the observations when the control effort U_s is applied accordingly.

The optimal solutions illustrated above depict the following observations when infectivity treatment is only applied.

(a) Figure 6 represents the effect of the control effort U_s on infectious drug sensitive (DS) strain of TB individuals. It implies that, the number of individuals will decrease to the minimum within 60 days if the control effort is optimally implemented in halting the disease's transmission.

(b) Figure 6 represents the effect of the control effort U_s on infectious drug resistant (DR) strain of TB individuals. It implies that, the number of individuals will decrease if the control effort is optimally implemented in halting the disease's transmission.

(c) Figure 6 represents the profile of control effort for tuberculosis cases finding. It implies that about 25% of all TB incidences should be found within 85 days and intensified in the subsequent days throughout the implementation.

Strategy 4: implementation of case holding (U_f)

The optimal solutions illustrated in Fig. 7 accounts the observations when the control efforts U_f is applied accordingly.

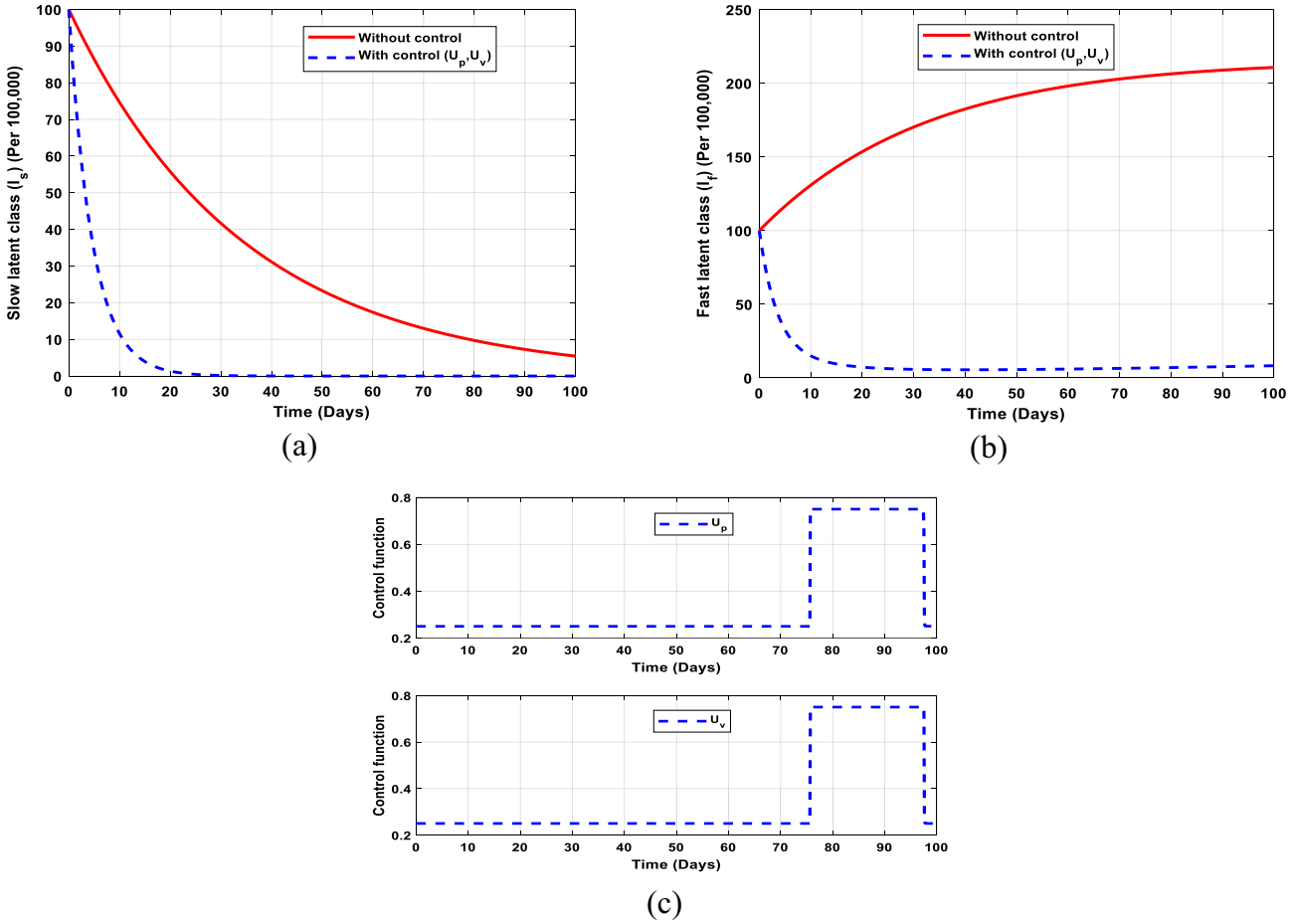

Fig. 8 Optimal solutions of implementing strategy 5

The optimal solutions illustrated above depict the following observations when control efforts for public awareness and vaccination are applied.

(a) Figure 7 represents the effect of the control effort U_f on infectious drug sensitive (DS) strain of TB individuals. It implies that, the number of individuals will decrease to the minimum within 80 days if the control effort is optimally implemented in halting the disease's transmission.
(b) Figure 7 represents the effect of the control effort U_f on infectious drug resistant (DR) strain of TB individuals. It implies that, the number of individuals will decrease if the control effort is optimally implemented in halting the disease's transmission.
(c) Figure 7 represents the profile of control effort for tuberculosis cases holding. It implies that about 50% of all TB incidences should be held with care especially, the drug-resistant strain of TB, throughout the implementation.

Strategy 5: implementation of public education and vaccination (U_p, U_v)

The optimal solutions illustrated in Fig. 8 accounts the observations when all the control efforts U_p, U_v are applied accordingly.

The optimal solutions illustrated above depict the following observations when all the control efforts for public awareness and infectivity treatment are applied.

(a) Figure 8 represents the effect of the control efforts U_p, U_v on infectious drug sensitive (DS) strain of TB individuals. It implies that, the number of individuals will decrease to the minimum within 20 days if the control efforts are optimally implemented in halting the disease's transmission.
(b) Figure 8 represents the effect of the control efforts U_p, U_v on infectious drug resistant (DR) strain of TB individuals. It implies that, the number of individuals

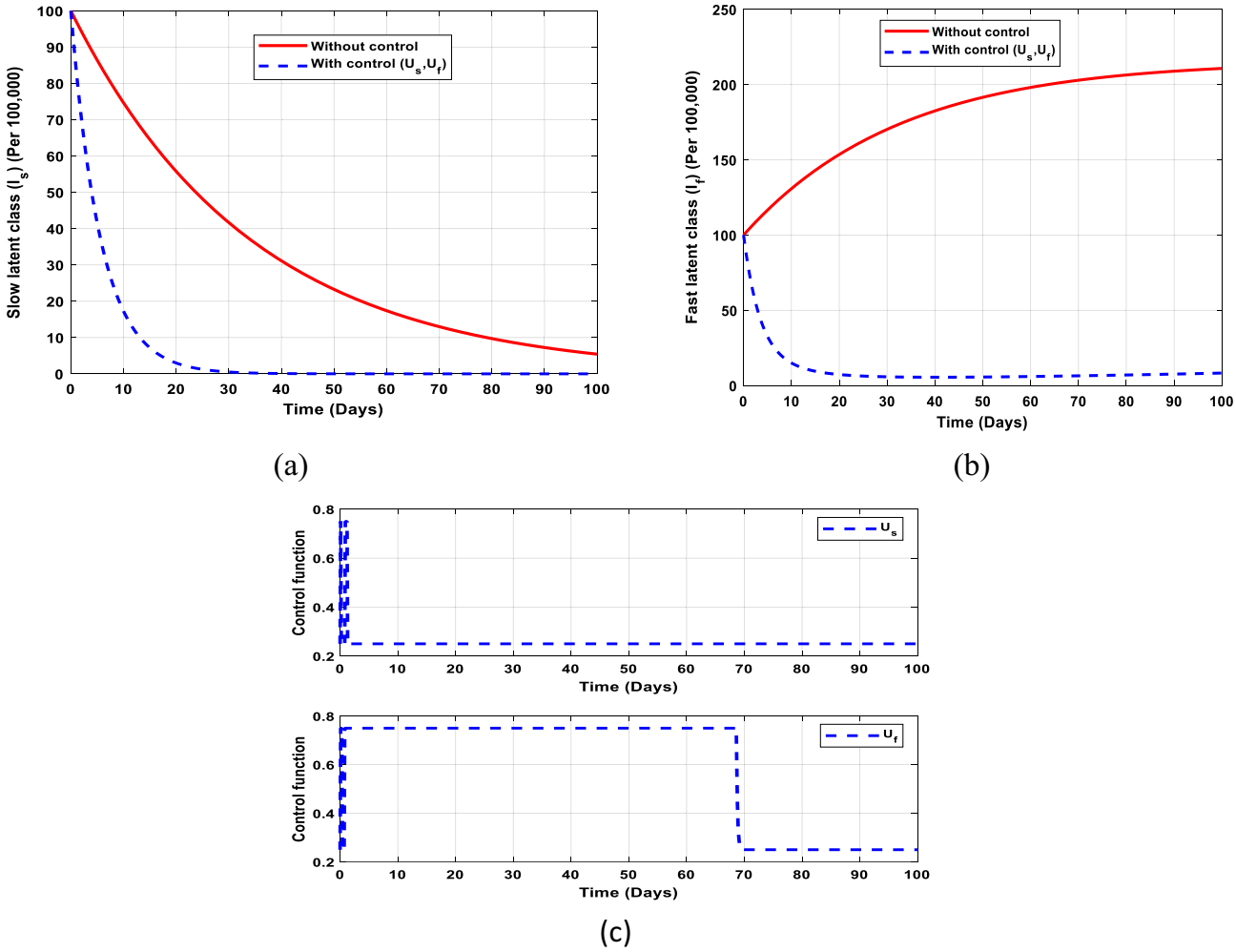

Fig. 9 Optimal solutions of implementing strategy 6

will decrease if the control effort is optimally implemented in halting the disease's transmission.

(c) Figure 8 represents the profile of control effort for tuberculosis cases holding. It implies that both vaccination and education on TB should reach about 25% of the population in 75 days and intensified to about 80% in the subsequent days throughout the implementation.

Strategy 6: implementation of case finding and case holding (U_s, U_f)

The optimal solutions illustrated in Fig. 9 accounts the observations when the control efforts U_s, U_f are applied accordingly.

The optimal solutions illustrated above depict the following observations when control efforts for case finding and case holding are applied.

(a) Figure 9 represents the effect of the control efforts U_s, U_f on infectious drug sensitive (DS) strain of TB individuals. It implies that, the number of individuals will decrease to the minimum within 30 days if the control efforts are optimally implemented in halting the disease's transmission.

(b) Figure 9 represents the effect of the control efforts U_s, U_f on infectious drug resistant (DR) strain of TB individuals. It implies that, the number of individuals will decrease if the control effort is optimally implemented in halting the disease's transmission.

(c) Figure 9 represents the profile of control effort for tuberculosis cases finding and case holding. It implies that about 80% of all TB incidences should be found form the beginning of the program. Also, about 80% of all the incidences should be held with care within 70 days throughout the implementation.

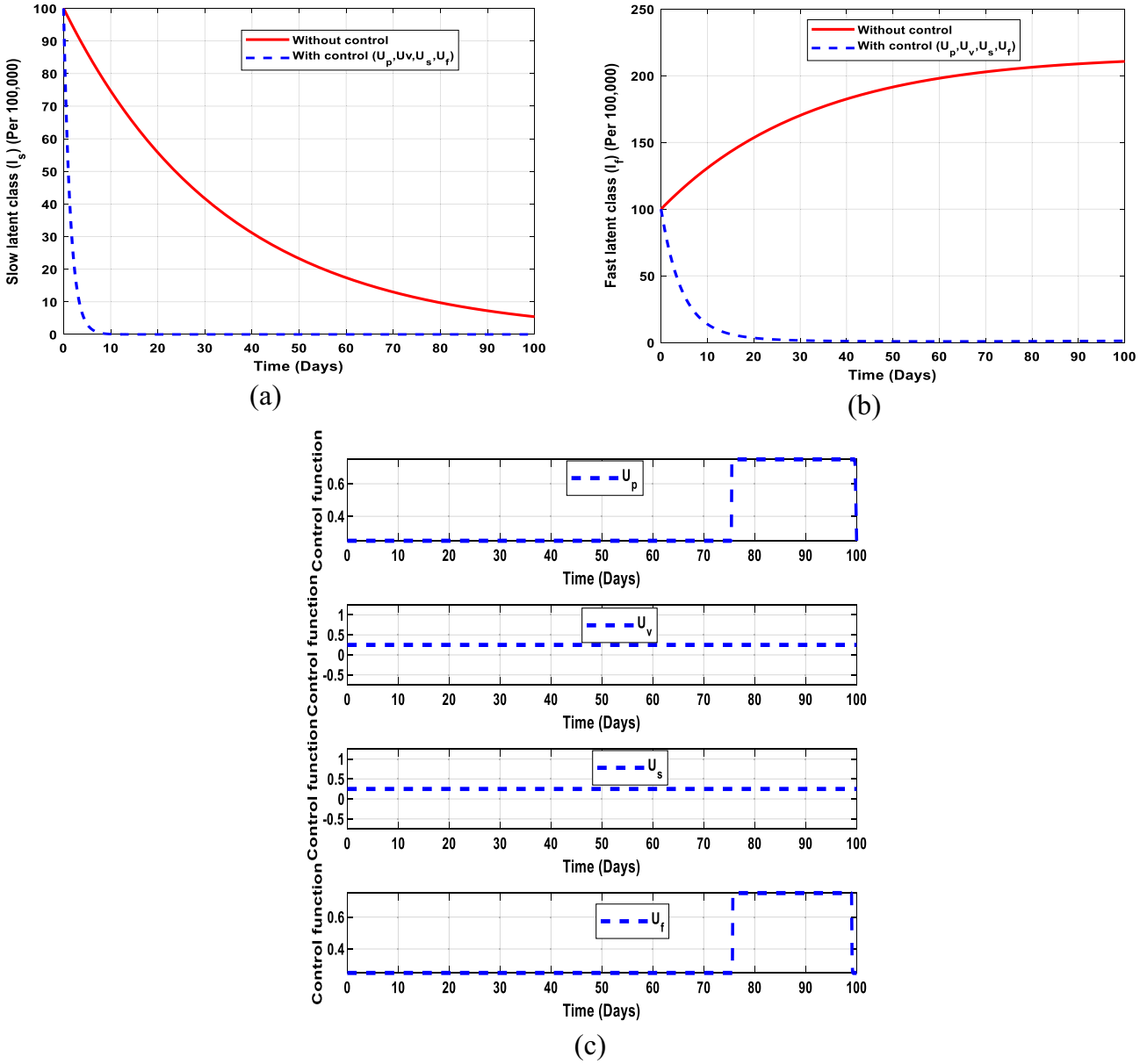

Fig. 10 Optimal solutions of implementing strategy 7

Table 2 Strategies' ACER values with their overall infection averted and cost incurred

Strategies	Overall infection averted	Overall cost involved	ACER value
Strategy 1	1.8069×10^{13}	177.6563	9.8321×10^{-12}
Strategy 2	3.0201×10^{13}	355.3125	1.1765×10^{-11}
Strategy 3	4.5571×10^{5}	715.6250	0.0016
Strategy 4	4.6474×10^{13}	700.7830	1.5079×10^{-11}
Strategy 5	3.0406×10^{13}	532.9688	1.7528×10^{-11}
Strategy 6	3.1416×10^{13}	2.5025×10^{3}	7.9657×10^{-11}
Strategy 7	4.8474×10^{13}	1.9494×10^{3}	4.0215×10^{-11}

Strategy 7: implementation of all controls (U_p, U_v, U_s, U_f)

The optimal solutions illustrated in Fig. 10 accounts the observations when the control efforts U_p, U_v, U_s, U_f are applied accordingly.

The optimal solutions illustrated above depict the following observations when all the control efforts applied.

(a) Figure 10 represents the effect of the control efforts U_p, U_v, U_s, U_f on infectious drug sensitive (DS) strain of TB individuals. It implies that, the number of individuals will decrease to the minimum within 10 days if the control efforts are optimally implemented in halting the disease's transmission.

(b) Figure 10 represents the effect of the control efforts U_p, U_v, U_s, U_f on infectious drug resistant (DR) strain of TB individuals. It implies that, the number of individuals will decrease if the control effort is optimally implemented in halting the disease's transmission.

(c) Figure 10 represents the profile of control efforts for tuberculosis education, vaccination, cases finding and case holding. It implies that both vaccination and TB incidence finding should be about 25% throughout the implementation. Also, 25% of the population should be educated on TB within 75 days and intensified up to 85% in the subsequent days. All TB cases should be held intensively up to 85% as well throughout the implementation.

Discussion

Cost-benefit analysis

Once the strategies are given, it's imperative to know the cost associated upon implementing such intervention(s). Therefore, we explore the cost associated with each control strategy to check their effectiveness. We layout some cost-effectiveness approaches to further understand the control strategies.

Table 3 Strategies' ICER values with their overall infection averted and cost incurred

Strategies	Overall infection averted	Overall cost incurred	ICER value
Strategy 3	4.5571×10^5	715.6250	0.0016
Strategy 1	1.8069×10^{13}	177.6563	-2.9773×10^{-11}
Strategy 2	3.0201×10^{13}	355.3125	1.4644×10^{-11}
Strategy 5	3.0406×10^{13}	532.9688	8.6662×10^{-10}
Strategy 6	3.1416×10^{13}	2.5025×10^3	1.9500×10^{-9}
Strategy 4	4.6474×10^{13}	700.7830	-1.1965×10^{-10}
Strategy 7	4.8474×10^{13}	1.9494×10^3	6.2431×10^{-10}

Table 4 Strategies' ICER values with their overall infection averted and cost incurred

Strategies	Overall infection averted	Overall cost incurred	ICER value
Strategy 1	1.8069×10^{13}	177.6563	9.8321×10^{-12}
Strategy 2	3.0201×10^{13}	355.3125	1.4644×10^{-11}
Strategy 5	3.0406×10^{13}	532.9688	8.6662×10^{-10}
Strategy 6	3.1416×10^{13}	2.5025×10^3	1.9500×10^{-9}
Strategy 4	4.6474×10^{13}	700.7830	-1.1965×10^{-10}
Strategy 7	4.8474×10^{13}	1.9494×10^3	6.2431×10^{-10}

Table 5 Strategies' ICER values with their overall infection averted and cost incurred

Strategies	Overall infection averted	Overall cost incurred	ICER value
Strategy 1	1.8069×10^{13}	177.6563	9.8321×10^{-12}
Strategy 5	3.0406×10^{13}	532.9688	2.8801×10^{-11}
Strategy 6	3.1416×10^{13}	2.5025×10^3	1.9500×10^{-9}
Strategy 4	4.6474×10^{13}	700.7830	-1.1965×10^{-10}
Strategy 7	4.8474×10^{13}	1.9494×10^3	6.2431×10^{-10}

Table 6 Strategies' ICER values with their overall infection averted and cost incurred

Strategies	Overall infection averted	Overall cost incurred	ICER value
Strategy 1	1.8069×10^{13}	177.6563	9.8321×10^{-12}
Strategy 6	3.1416×10^{13}	2.5025×10^{3}	1.7418×10^{-10}
Strategy 4	4.6474×10^{13}	700.7830	-1.1965×10^{-10}
Strategy 7	4.8474×10^{13}	1.9494×10^{3}	6.2431×10^{-10}

Table 7 Strategies' ICER values with their overall infection averted and cost involved

Strategies	Overall infection averted	Overall cost incurred	ICER value
Strategy 1	1.8069×10^{13}	177.6563	9.8321×10^{-12}
Strategy 4	4.6474×10^{13}	700.7830	1.8417×10^{-11}
Strategy 7	4.8474×10^{13}	1.9494×10^{3}	6.2431×10^{-10}

Table 8 Strategies' ICER values with their overall infection averted and cost incurred

Strategies	Overall infection averted	Overall cost incurred	ICER value
Strategy 1	1.8069×10^{13}	177.6563	9.8321×10^{-12}
Strategy 7	4.8474×10^{13}	1.9494×10^{3}	5.8271×10^{-11}

We consider two procedures namely; Average cost-effectiveness ratio (ACER) and Incremental cost-effectiveness ratio (ICER), which have been as explained in (Osei et al. 2023; Asamoah et al. 2020; Agusto and Leite 2017; Asamoah et al. 2022) to carry out epidemiological studies.

The average cost-effectiveness ratio (*ACER*)

We define the average cost-effectiveness ratio (ACER) of implementing a strategy as;

$$\text{ACER} = \frac{\text{Overall cost generated by applying the strategy}}{\text{Overall infection averted by applying the strategy}}. \tag{41}$$

The overall cost is M, stated in Eq. (33) would be used to evaluate the total cost that the intervention would generate. We then compare the ACER values of each strategy, the one with least value saves cost. Therefore, the cost-effective intervention is considered as the strategy with the least ACER value. This is illustrated below.

From Table 2, control strategy 1, thus the implementation of public education only has the least value of ACER, hence saves cost. This is not enough to choose a strategy; we further explore other approach.

The incremental cost-effectiveness ratio (ICER)

We define the incremental cost-effectiveness ratio (ICER) of implementing a strategy as;

$$\text{ICER} = \frac{\text{The cost difference generated by strategies } x \text{ and } y}{\text{Difference in the overall infection averted in strategies } x \text{ and } y}. \tag{44}$$

The total cost function M, stated in Eq. (33) would be used to estimate the overall cost that the intervention would generate. It is worth knowing that, the averted total number of infections is the difference between the initial values of E_x, I_x, without control(s) and with controls. The outcomes are tabulated below in infection averted increasing order.

The ICER in Table 3 is calculated as:

$$\text{ICER}(3) = \frac{715.6250 - 0}{4.5571 \times 10^{5} - 0} = 0.0016,$$

$$\text{ICER}(1) = \frac{177.6563 - 715.6250}{1.8069 \times 10^{13} - 4.5571 \times 10^{5}} = -2.9773 \times 10^{-11},$$

$$\text{ICER}(2) = \frac{355.3125 - 177.6563}{3.0201 \times 10^{13} - 1.8069 \times 10^{13}} = 1.4644 \times 10^{-11},$$

$$\text{ICER}(5) = \frac{532.9688 - 355.3125}{3.0406 \times 10^{13} - 3.0201 \times 10^{13}} = 8.6662 \times 10^{-10},$$

$$\text{ICER}(6) = \frac{2.5025 \times 10^{3} - 532.9688}{3.1416 \times 10^{13} - 3.0406 \times 10^{13}} = 1.9500 \times 10^{-9},$$

$$\text{ICER}(4) = \frac{700.7830 - 2.5025 \times 10^{3}}{4.6474 \times 10^{13} - 3.1416 \times 10^{13}} = -1.1965 \times 10^{-10},$$

$$\text{ICER}(7) = \frac{1.9494 \times 10^{3} - 700.7830}{4.8474 \times 10^{13} - 4.6474 \times 10^{13}} = 6.2431 \times 10^{-10}.$$

Focusing on strategy 3 and strategy 1 in Table 3, it is noticed from the ICER that, strategy 3 is expensive to deploy in a resource limited setting, therefore, strategy 3 is removed from the list of possible controls and the ICER is calculated again. This is presented in Table 4.

Focusing on strategy 1 and strategy 2 in Table 4, it is noticed from the ICER that, strategy 2 is expensive to deploy in a resource limited setting, therefore, strategy 2 is dropped from the list of possible controls and the ICER is calculated again. This is presented in Table 5.

Focusing on strategy 1 and strategy 5 in Table 5, it is noticed from the ICER that, strategy 5 is expensive to deploy in a resource limited setting, therefore, strategy 5 is dropped from the list of possible controls and the ICER is calculated again. This is presented in Table 6.

Focusing on strategy 1 and strategy 6 in Table 6, it is noticed from the ICER that, strategy 6 is expensive to deploy in a resource limited setting, therefore, strategy 6 is dropped from the list of possible controls and the ICER is calculated again. This is presented in Table 7.

Focusing on strategy 1 and strategy 4 in Table 7, it is noticed from the ICER that, strategy 4 is expensive to deploy in a resource limited setting, therefore, strategy 4 is dropped from the list of possible controls and the ICER is calculated again. This is presented in Table 8.

Finally, assessing strategy 1 and strategy 7 in Table 8, it is noticed from the ICER that, strategy 7 is expensive to deploy in a resource limited setting, therefore, strategy 7 is removed from the list of possible controls. Therefore, we conclude that strategy 1 is the most cost-effective strategy to use among the several strategies under study here. From the above analysis, it is obvious that strategy 1, thus; public education is the intervention that saves cost.

Conclusion

We have presented an epidemiological model incorporating two latent classes using ordinary differential equations to explore the transmission dynamics of tuberculosis (TB) using data from Ghana. We estimated the model's parameters and analyzed their effects on the disease's transmission through numerical and graphical illustrations. Again, we elaborated the threshold dynamics of the effective reproduction number R_e by evaluating the reproduction numbers of the two latent classes. It was observed that the reproduction number of the slow latent class with drug-sensitive (DS) strain of TB, $R_s = 0.27$ and the reproduction number of the fast latent class with drug-resistant (DR) strain of TB $R_f = 2.23$. This signifies that, about 10.8% of the reported cases are associated DS strain of TB whiles 89.2% of the reported cases are associated DR strain of TB. It is obvious that treatment of TB is not easy due to ineffective vaccine as explained in (Chaulet 1983; Reichman and Hershfield 2000).

Our goal is to mitigate the transmission of the tuberculosis; therefore, we formulated an optimum strategy that considers control measures with both pharmaceutical and non-pharmaceutical to control both strains of TB infection. We implemented the strategies (see Figs. 4, 5, 6, 7, 8, 9, 10) and it is observed that, public education on prevention of TB should be intensified and reach about 100% of the population, vaccination should be enhanced and vaccinate about 25% of newborns at any given time, case holding and case finding as explained in (Nsanzumuhirc et al. 1981) needs about 75% enforcement because they are helpful in controlling the spread of TB. This indicates that, although vaccination is good but it largely depends on the rising of the drug-resistant (DR) strain infections if failure of treatment of individuals infectious with drug-sensitive (DS) strain occur. We further encourage the health service to enhance the mechanism for TB diagnosis by following the recommendation in (CDC 2014).

It is also worth knowing that public education saves cost per the cost-effectiveness analysis compared to the other strategies raised in this work. This intervention can minimize TB as illustrated in Fig. 4. This intervention should reach about 75% of the population from the beginning and intensified in the subsequent days in order to realize the results of strategy 1 (see Fig. 4). However, it's imperative to check the effectiveness and cost of all the strategies raised in this work when choosing a control measure (see Tables 2, 3, 4, 5, 6, 7, 8).

The outcomes of the findings imply that, non-pharmaceutical measures such as public education on prevention of TB is very important in controlling the transmission of TB. This control measure should be vigorous always to create public awareness on TB as illustrated in Fig. 3 to reduce the effective contact rate and rate of acquiring the TB. The pharmaceutical measures such as vaccination against TB etc. is important however, it should be implemented with vigilance because of the existence of drug-resistant (DR) strain. This control measure should be mild as illustrated in Fig. 5, with keen observation of public education.

In the nut shell, research conducted without considering the strains of TB in Ashanti region, Ghana reveals the possibility of TB becoming endemic in some districts (Okoe et al. 2020). We have modelled the transmission of TB in Ghana incorporating two strains to determine the main source of transmission and minimized the transmission of the disease by implementing optimum strategies. The findings of this research depict the situation of TB transmission in Ghana and applicable to other countries with similar phenomena. Therefore, we encourage the Ghana health service to be keen on observing drug-resistant (DR) strain of TB since it has higher infection rate compared to drug-sensitive (DS)

strain of TB. Also, people infected with either strain of TB are advised to complete their prophylaxis to help halt the transmission of TB. We hope to extend this study to explore the transmission of TB by considering heterogeneity such as age, sex etc., since our modeling approach is limited to population homogeneity.

Author contributions Raymond Fosu Appiah: Conceptualization, investigation, formal analysis, writing, review and editing. Zhen Jin: Supervision, review, editing and funding acquisition. Junyuan Yang: Supervision, formal analysis, review and editing. Joshua Kiddy K. Asamoah: Investigation, review and editing.

Data availability The authors confirm that the data supporting the findings of this study are available within the article.

Declarations

Conflict of interest We declare that there are no known personal relationships or financial interests that could affect the findings presented in this paper.

References

Abidemi A, Fatoyinbo HO, Asamoah JKK & Muni SS (2022) Evaluation of the efficacy of Wolbachia intervention on dengue burden in a population: a mathematical insight. In: 2022 International Conference on Decision Aid Sciences and Applications (DASA) IEEE. pp 1618–1627. https://doi.org/10.1109/DASA54658.2022.9765106

Addai E, Adeniji A, Ngungu M et al (2023) A nonlinear fractional epidemic model for the Marburg virus transmission with public health education. Sci Rep 13:19292. https://doi.org/10.1038/s41598-023-46127-7

Addai E, Torres DFM, Abdul-Hamid Z et al (2024) Modelling the dynamics of online food delivery services on the spread of foodborne diseases. Model Earth Syst Environ. https://doi.org/10.1007/s40808-024-02046-8

Adebisi YA, Agumage I, Sylvanus TD et al (2019) Burden of tuberculosis and challenges facing its eradication in West Africa. Int J Infect. https://doi.org/10.5812/iji.92250

Adu IK, Wireko FA, Nana-Kyere S et al (2024) Modelling the dynamics of Ebola disease transmission with optimal control analysis. Model Earth Syst Environ. https://doi.org/10.1007/s40808-024-02020-4

Agusto F, Leite M (2017) mOptimal control and cost-effective analysis of the meningitis outbreak in Nigeria. Infect Dis Model 4(2019):161–187

Appiah RF, Jin Z, Yang J, Asamoah JKK, Wen Y (2024a) Mathematical modeling of two strains tuberculosis and COVID-19 vaccination model: a co-infection study with cost-effectiveness analysis. Front Appl Math Stat 10:1373565. https://doi.org/10.3389/fams.2024.1373565

Appiah RF, Jin Z, Yang J, Asamoah JKK (2024b) Cost–benefit analysis of the COVID-19 vaccination model incorporating different infectivity reductions. Front Phys 12:1383357. https://doi.org/10.3389/fphy.2024.1383357

Asamoah JKK, Owusu MA, Jin Z, Oduro FT, Abidemi A, Gyasi EO (2020) Global stability and cost-effectiveness analysis of COVID-19 considering the impact of the environment: using data from Ghana. Chaos Solitons Fractals 140:110103. https://doi.org/10.1016/j.chaos.2020.110103

Asamoah JKK, Okyere E, Abidemi A, Moore SE, Sun G, Jin Z, Acheampong E, Gordon JF (2022) Optimal control and comprehensive cost-effectiveness analysis for COVID-19. Results Phys 33:105177. https://doi.org/10.1016/j.rinp.2022.105177

Asamoah JKK, Safianu B, Afrifa E, Obeng B, Seidu B, Wireko FA, Sun GQ (2023) Optimal control dynamics of Gonorrhea in a structured population. Heliyon. https://doi.org/10.1016/j.heliyon.2023.e20531

Blower SM, Gerberding J (1998) Understanding, predicting and controlling the emergence of drug-resistant tuberculosis: a theoretical framework. J Mol Med 76:624–636

Blower SM, Small PM, Hopewell PC (1996) Control strategies for tuberculosis epidemics: new models for old problems. Science 273:497–500

Blower SM, Porco T, Lietman T (1998) Tuberculosis: The evolution of antibiotic resistance and the design of epidemic control strategies. In: Horn, Simonett, Webb (eds) Mathematical models in medical and health sciences. Vanderbilt University Press

Castillo-Chavez C, Feng Z (1997) To treat or not to treat: the case of tuberculosis. J Math Biol 35:629–659

Castillo-Chavez C, Feng Z (1998) Global stability of an age-structure model for TB and its applications to optimal vaccination strategies. Math Biosci 151:135–154

Castillo-Chavez C, Song B (2004) Dynamical models of tuberculosis and their applications. Math Biosci Eng 1(2):361–404

CDC, Center for Disease Control (2014) Latent tuberculosis infection: a guide for primary health care providers. CDC, Atlanta

Chaulet P (1983) Treatment of tuberculosis: case holding until cure, WHO/TB/83. World Health Organization, Geneva, p 14

Dontwi I, Obeng-Denteh W, Andam E (2014) A mathematical model to predict the prevalence and transmission dynamics of tuberculosis in Amansie West district, Ghana. Br J Math Comput Sci 4(3):402–425

Fister KR, Lenhart S, McNally JS (1998) Optimizing chemotherapy in an HIV model. Electron J Differ Equ 1998(32):1–12

Gomes M, Gabriela M, Franco AO, Gomes MC, Medley GF (2004) The reinfection threshold promotes variability in tuberculosis epidemiology and vaccine efficacy. Proc R Soc Lond B 271:617–623

Hale JK, Waltman P (1981) Persistence in finite dimensional systems. SIAM J Math Anal 20:388–395

He R, Luo X, Asamoah JKK et al (2023) A hierarchical intervention scheme based on epidemic severity in a community network. J Math Biol 87:29. https://doi.org/10.1007/s00285-023-01964-y

Hethcote HW (2000) The mathematics of infectious diseases. SIAM Rev 42(4):599–653

Kirschner DS, Lenhart, Serbin S (1997) Optimal control of the chemotherapy of HIV. J Math Biol 35:775–792

Li G, Jin Z (2005) Global stability of a seir epidemic model with infectious force in latent, infected and immune period. Chaos Solitons Fractals 25(5):1177–1184

Li MY, Muldowney JS (1995) Global stability for the seir model in epidemiology. Math Biosci 125(2):155–164

Mettle FO, Affi PO, Twumasi C (2020) Modeling the transmission dynamics of tuberculosis in the Ashanti Region of Ghana. Interdisciplin Perspect Infect Dis 2020:16 (**Article ID 4513854**)

Moore SE, Nyandjo-Bamen HL, Menoukeu-Pamen O, Asamoah JKK, Jin Z (2022) Global stability dynamics and sensitivity assessment of COVID-19 with timely-delayed diagnosis in Ghana. Comput Math Biophys 10(1):87–104. https://doi.org/10.1515/cmb-2022-0134

Nsanzumuhirc H et al (1981) A third study of case-finding methods for pulmonary tuberculosis in Kenya, including the use of community leaders. Tubercle 62:79–94

Osei E, Amu H, Kye-Duodu G, Kwabla MP, Danso E, Binka FN et al (2023) Impact of COVID-19 pandemic on Tuberculosis and HIV services in Ghana: an interrupted time series analysis. PLoS One 18(9):e0291808. https://doi.org/10.1371/journal.pone.0291808

Reichman LB, Hershfield ES (2000) Tuberculosis: a comprehensive international approach. Dekker, New York

Ren H, Xu R (2024) Prevention and control of Ebola virus transmission: mathematical modelling and data fitting. J Math Biol 89:25. https://doi.org/10.1007/s00285-024-02122-8

Rieder HL et al (1989) Epidemiology of tuberculosis in the United States. Epidemiol Rev 11:89–95

Rwezaura H, Diagne M, Omame A, de Espindola A, Tchuenche J (2022) Mathematical modeling and optimal control of SARS-CoV-2 and tuberculosis co-infection: a case study of Indonesia. Model Earth Syst Environ 8(4):5493–5520

Seidu B, Wiah EN, Asamoah JKK (2023) Optimal strategies for control of cholera in the presence of hyper-infective individuals. Result Phys 53:106968. https://doi.org/10.1016/j.rinp.2023.106968

Shuai Z, van den Driessche P (2013) Global stability of infectious disease models using Lyapunov functions, SIAM. J Appl Math 73:1513–1532. https://doi.org/10.1016/10.1137/120876642

Snider DE Jr, Raviglione M and Kochi A (1994) Global burden of tuberculosis," in Tuberculosis, pp. 3–11, American Society for Microbiology (ASM), Washington, DC, US

Trauer JM, Denholm JT, McBryde ES (2014) Construction of a mathematical model for tuberculosis transmission in highly endemic regions of the Asia-pacific. J Theor Biol 358:74–84

Van den Driessche P, James W (2002) Reproduction numbers and subthreshold endemic equilibria for compartmental models of disease transmission. Math Biosci 180:29–48

Wang X, Li J, Guo S et al (2023) Dynamic analysis of an Ebola epidemic model incorporating limited medical resources and immunity loss. J Appl Math Comput 69:4229–4424. https://doi.org/10.1007/s12190-023-01923-2

WHO, World Health Organization (2018) Ghana-Incidence of Tuberculosis (Per 100,000 People)-1990–2018 Data-2020 Forecast, World Health Organization, Geneva, Switzerland

WHO, World Health Organization (2023) Global Tuberculosis Report. Incidence of tuberculosis (per 100,000 people) - Ghana | Data (worldbank.org) Geneva, Switzerland

WHO, World Health Organization, Global Tuberculosis Report (2013) World Health Organization, Geneva, Switzerland

WHO, World Health Organization, Global Tuberculosis Report (2016), World Health Organization, Geneva, Switzerland

WHO, World Health Organization, World Health Statistics (2015) World Health Organization, Geneva, Switzerland

Wireko FA, Asamoah JKK, Adu IK, Ndogum S (2024) Non-optimal and optimal fractional control analysis of measles using real data. Inform Med Unlocked. https://doi.org/10.1016/j.imu.2024.101548

Zhilan F, Castillo-Chavez C, Capurro AF (2000) A model for tuberculosis with exogenous reinfection. Theoretical 57(3):235–247